Renewable and Sustainable Energy Reviews 32 (2014) 739–761

Contents lists available at ScienceDirect

Renewable and Sustainable Energy Reviews

journal homepage: www.elsevier.com/locate/rser

A review of hydrogen and natural gas addition in diesel HCCI engines

A. Aziz Hairuddin [a,c,*], Talal Yusaf [b], Andrew P. Wandel [a]

[a] Computational Engineering and Science Research Centre, University of Southern Queensland, Toowooomba, 4350 QLD, Australia
[b] National Centre for Engineering in Agriculture, University of Southern Queensland, Toowooomba, 4350 QLD, Australia
[c] Department of Mechanical and Manufacturing Engineering, Universiti Putra Malaysia, 43400 UPM Serdang, Selangor, Malaysia

ARTICLE INFO

Article history:
Received 18 December 2012
Received in revised form
29 November 2013
Accepted 4 January 2014
Available online 11 February 2014

Keywords:
HCCI
Engine
Hydrogen
Natural gas
Diesel
Numerical
Chemical kinetic

ABSTRACT

Homogeneous charge compression ignition (HCCI) engine uses a relatively new mode of combustion technology. In principle, there is no spark plug or injector to assist the combustion, and the combustion auto-ignites in multiple spots once the mixture has reached its chemical activation energy. The challenges in developing HCCI engines are the difficulties in: controlling the auto-ignition of the mixture and the heat release rate at high load operations, achieving a cold start, meeting emission standards and controlling knock. At low engine speeds, early auto-ignition can occur, possibly leading to knocking, while late auto-ignition at high engine speeds will make HCCI susceptible to misfire. Hydrogen greatly reduces emissions levels but with reduced power. However, when hydrogen is combined with diesel in dual-fuel mode, low NO_x, CO and particulate matter (PM) emissions levels can be achieved, and engine efficiency can be increased by 13–16%. Numerical methods are commonly used to predict HCCI engines′ performance (i.e. emissions levels, brake thermal efficiency and combustion phasing), which is cost-effective compared to solely relying on experimentation. The multi-zone method promises better simulation results compared to the single-zone model by combining detailed chemical kinetics with simplified 3D modeling so that turbulence and inhomogeneity in the mixture are considered; good agreement between simulations and experiments have been achieved. Specific strategies used in the experimental method (e.g. fuel additives, inlet air heating, inlet air pressurizing, exhaust gas recirculation (EGR) and injection methods), and numerical method (e.g. single-zone and multi-zone models, mixing model, turbulence model and multi-dimensional model), and other issues associated with HCCI engines are discussed in this paper.

Contents

* Corresponding author at: Computational Engineering and Science Research Centre, University of Southern Queensland, Toowooomba, 4350 QLD, Australia.
E-mail address: Ahziz@upm.edu.my (A.A. Hairuddin).

1364-0321/$ - see front matter
http://dx.doi.org/10.1016/j.rser.2014.01.018

1. Introduction

Internal combustion (IC) engines are widely used in numerous applications throughout the world. A new mode of combustion is being sought in order to reduce the emissions levels from these engines: homogeneous charge compression ignition (HCCI) engine technology is a potential candidate. The HCCI technique is the process by which a homogeneous mixture of air and fuel is compressed until auto-ignition occurs near the end of the compression stroke, followed by a combustion process that is significantly faster than either Compression Ignition (CI) or Spark Ignition (SI) combustion [1]. HCCI technology claimed to improve the engine thermal efficiency while maintaining low emissions and can be implemented by modifying either SI or CI engines using any fuel or combination of fuels [2,3]. The air/fuel mixture quality in HCCI engines is normally lean, it auto-ignites in multiple locations and is then burned volumetrically without discernible flame propagation [4]. Combustion takes place when the homogeneous fuel mixture has reached the chemical activation energy and is fully controlled by chemical kinetics [5] rather than spark or injection timing.

Since the mixture is lean and it is fully controlled by chemical kinetics, there are new challenges in developing HCCI engines as it is difficult to control the auto-ignition of the mixture and the heat release rate at high load operation, achieve cold start, meet emission standards and control knock [6,7]. The advantages of using HCCI technology in IC engines are: (1) high efficiency relative to SI engines – approaching the efficiency of CI engines due to the ability of these engines to high compression ratio (CR) and fast combustion [8,9]; (2) the ability to operate on a wide range of fuels [9–11]; and (3) the ability to be used in any engine configuration: automobile engines, stationary engines, heavy duty engines or small sized engines [2,12,13]. On the other hand, HCCI engines have some disadvantages such as high levels of unburned hydrocarbons (UHC) and carbon monoxide (CO) [6,14,15] as well as knocking under certain operating conditions [6,14,16].

Emissions regulations are becoming more stringent and NO_x and soot emissions levels in HCCI engines have been greatly reduced without sacrificing efficiency, which is close to that of CI engines [14]. However, knocking is still the major issue because of its sudden onset. Knocking is due to premature combustion where the ignition takes place before the piston reaches top dead center (TDC) and it reduces engine's reliability due to high vibration effects.

The performance of an HCCI engine is strongly dependent on the fuel type, and this affects the emissions levels as well. Since the emissions levels become one of the factors driving engine technology today, HCCI development has moved to a next level. Due to the importance of HCCI technology, which potentially can replace the conventional SI and CI engines, there is a need to report the recent development of HCCI engines. This paper discusses the current issues for this technology. It consists of six sections, where Section 2 contains the performance comparison between natural gas and hydrogen in HCCI mode. Section 3 presents the methods to create homogeneous mixtures, with ignition control of HCCI engines in Section 4. Section 5 will discuss relevant numerical studies, concluding with Section 6.

2. Performance comparison

2.1. State of the art current internal combustion engines

Producing homogenous mixtures to achieve near-complete combustion is a common goal that will lead to the development of low polluting engines. Some technologies include Fuel-Stratified Injection (FSI), Turbo-Stratified Injection (TSI) and HCCI. All these technologies (FSI, TSI, and HCCI) are used to improve the combustion efficiencies by introducing a homogeneous mixture inside the combustion chamber.

FSI and TSI are commercially used by the Volkswagen Aktiengesellschaft (AG), which consists of other child companies: Audi, Skoda, Seat, Bugatti, Lamborghini, Bentley and Scania [17]. FSI uses direct injection fuel with high injection pressure, where the evaporating fuel has a significant cooling effect on the cylinder charge [18]. This effect helps in reducing the knock and therefore higher compression ratio can be used. The air enters the combustion chamber at a certain angle by using a moveable flap inside the intake manifold, while fuel is directly injected during the intake stroke. The fuel injector is located close to the inlet valve in the cylinder head. With the help of the piston crown design, the air will experience tumbling effects inside the chamber. This in turn will help the fuel mix with air homogeneously.

TSI engines, on the other hand, implement a high intake pressure (using multipoint injectors) on an FSI engine. This allows the fuel to mix homogeneously with the air during the compression stroke. Furthermore, pressurizing the intake air will assist the combustion and therefore produce better efficiency, allowing smaller engines to be built with power and torque similar to that of bigger engines. The first engine uses direct injection technology to stratified charge engine was the Texaco combustion process [19], as reported by [20].

HCCI engines can be considered as new technology even though the research was initially undertaken by Onishi et al. in

1979, as reported in [21]. Researchers worldwide are investigating HCCI engines as this technology has not yet been sufficiently developed and commercially available. They can be used in either SI or CI engine configurations with a high CR. HCCI engines operate without using diesel injectors or spark plugs and high efficiency can be achieved with low NO_x and soot emissions. General Motors (GM) corporation has unveiled a prototype car with a gasoline HCCI engine, which could cut fuel consumption by 15% [22]. The engine is able to virtually eliminate NO_x emissions and lower throttling losses, which improves fuel economy.

2.2. Fuels used in HCCI engines

HCCI engines can operate using any fuel as long as the fuel can be vaporized and mixed with the air before ignition [10]. Since HCCI engines are fully controlled by chemical kinetics, it is important to evaluate the fuel's auto-ignition point to produce smooth engine operation: no knocking or misfiring. Different fuels will have different auto-ignition points. Fig. 1 shows the intake temperature required for different fuels to auto-ignite at difference compression ratios when operating in HCCI mode [10]. It is clearly seen that methane requires a high intake temperature and high compression ratio to auto-ignite. The auto-ignition point decreases when the number of carbon atoms in the hydrocarbon increases, as shown in Fig. 1, where methane has the fewest possible carbon atoms, while *iso*-octane has the most of those shown.

The compositions of natural gas vary for different countries as shown in Table 1. It is easily adapted for use as a fuel due its wide

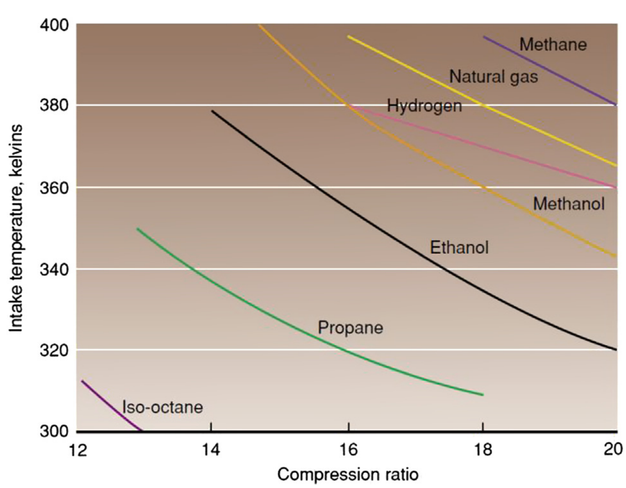


Fig. 1. Intake temperature required for fuels to operate under HCCI mode with varying compression ratios, reproduced from [10].

Table 1
The difference in natural gas composition between some countries [4,23,35–38].

Components	%Volume				
	Australia	*Greece*	*Sweden*	*US*	*Malaysia*
Methane (CH_4)	90.0	98.0	87.58	91.1	92.74
Ethane (C_2H_6)	4.0	0.6	6.54	4.7	4.07
Propane (C_3H_8)	1.7	0.2	3.12	1.7	0.77
Butane (C_4H_{10})	0.4	0.2	1.04	1.4	0.14
Pentane (C_5H_{12})	0.11	0.1	0.17	–	–
Hexane (C_6H_{14})	0.08	–	0.02	–	–
Heptane (C_7H_{16})	0.01	–	–	–	–
Carbon dioxide (CO_2)	2.7	0.1	0.31	0.5	1.83
Nitrogen (N_2)	1.0	0.8	1.22	0.6	0.45

Table 2
Natural gas emissions levels compared to oil and coal (Pounds per billion Btu of energy) [24].

Pollutant	Natural gas	Oil	Coal
Carbon dioxide	117,000	164,000	208,000
Carbon monoxide	40	33	208
Nitrogen oxides	92	448	457
Sulfur dioxide	0.6	1122	2591
Particulates	7.0	84	2744
Mercury	0.000	0.007	0.016

availability, is economic and has environmental benefits because it produces fewer emissions than crude oil and coal, as illustrated in Table 2 [23,24]. It can be seen that crude oil and coal produced carbon dioxide at a rate approximately 1.4 to 1.75 times higher than natural gas. Natural gas is also more readily available than crude oil, with a cost that has been competitive for a long time [25]. Natural gas is able to operate as a single fuel in an IC engine with low HC and CO emissions, however it suffers less power output in HCCI engines [26–28]. Its high auto-ignition point (about 810 K) gives it a significant advantage over diesel–natural gas operation by maintaining the high CR of a diesel engine and lowering emissions at the same time [23,29,30]. Duc and Wattanavichien [29] claimed that the high octane number of methane (about 120) allows engines to operate at a high CR. Results from a four-stroke HCCI engine simulation have shown that methane did not ignite if the intake temperature was less than 400 K with a CR of 15:1, as reported by [31]. This is supported by Fig. 1, where methane will only auto-ignite with an intake temperature less than 400 K when CR is greater than 18:1.

Car manufacturers are producing cars powered by fuel-cells, as well as engines operated with compressed natural gas (CNG) [32,33]. They are purpose-built to reduce emissions and are more economical than gasoline and diesel. There are commercialization difficulties for fuel-cells because of their complexity to produce and safety issues. CNG on the other hand has been successfully commercialized with 48% of the global market share, but it has difficulties with high capital cost, existing refueling infrastructure and competition from other alternative fuels [34].

The Indicated Mean Effective Pressure (IMEP) is a measure of the engine's capacity to do work in each stroke, before considering all the losses. If IMEP is increased, it can reduce the intake temperature needed in an HCCI engine; increasing the CR has the same effect [36]. Antunes, Mikalsen and Roskilly [39] have investigated the engine performance of an HCCI engine fueled with hydrogen, and they found that the IMEP increases when the air intake temperature is decreased. Hydrogen requires a lower air intake temperature than natural gas for the same CR, as shown in Fig. 1, due to hydrogen having a lower density. Therefore, it is important to control the intake temperature and the operating conditions of an HCCI engine to achieve an optimized combustion point and the methods to achieve this will be discussed in Sections 3 and 4.

Hydrogen can operate as a single fuel in an HCCI engine but it is often unstable and is prone to generate knocking [40]. It has the highest diffusivity of any gas in air, about 3–8 times faster than that of natural gas, which leads to fast mixing [30] and the intake charge can be considered homogeneous when premixed with air [40]. The net heating value for hydrogen is almost three times higher than diesel (119.93 MJ/kg compared to 42.0035 MJ/kg) with a high self-ignition temperature to initiate combustion (858 K) [41]. Since hydrogen cannot be stably used as a single fuel in an HCCI engine, most researchers use it as an additive: either to control the ignition timing or to increase the engine performance [1,26,30,42,43].

Iso-octane is used as a surrogate fuel for gasoline in HCCI engine experiments while *n*-heptane is used for diesel [44–46]. Alcohol-derived fuels, as shown in Fig. 1, are not widely used due to their complexity to produce, leading to high manufacturing costs. Most of the alcohol-derived fuels like biofuels are still subject to worldwide investigations as they create clogging issues in the engine. Even though biofuels have their own challenge, they have received increasing attention from researchers as a renewable source, as reported by [47].

2.3. Natural gas and hydrogen operating conditions

The combination of Natural gas or hydrogen with diesel reported to yield low emissions and to some extent increase the engine efficiency, either in HCCI or CI combustion mode [41,48–50]. Diesel alone is not suitable for HCCI engines due to its low volatility and high propensity to auto-ignite while natural gas has a high resistance to auto-ignition as reported by [51].

Combinations of high octane number fuels (such as natural gas and hydrogen) with high cetane number fuels (such as diesel) are able to increase the engine durability, and under certain operating conditions reduce emissions levels such as soot, HC, CO and NO_x [40,52–54]. It was also reported that these combinations have a high thermal efficiency under early injection timing [52,54]. Fuels with a higher octane number have better resistance to knocking while fuels with a higher cetane number have a shorter ignition delay time, thus providing more time for the fuel to complete the combustion. Therefore, a combination of both (high cetane number fuels and high octane number fuels) provides soft engine run [40], whereby the mixture can be operated at high CR and has longer combustion duration.

Hydrogen has a high octane number (about 130) as well as a high lower heating value (LHV) (119.93 MJ/kg) and its combination with diesel helps to increase engine efficiency and control the auto-ignition point in HCCI engines. Natural gas, on the other hand, has a high auto-ignition temperature and it can be used in high CR engines. Table 3 compares the physical and chemical properties of diesel with natural gas and hydrogen.

Hydrogen has the highest LHV or Lower Calorific Value (LCV) compared to both diesel and natural gas, which means that it releases a high amount of energy during combustion and thus produces the highest flame speed. The wide range of the flammability limits allows a wide range of engine power outputs through changes in the mixture equivalence ratio. Flammable mixtures of hydrogen can go from as lean as $\lambda = 10$ to as rich as $\lambda = 0.14$ [50], where λ is the air-to-fuel ratio.

Table 3
Diesel properties compared to hydrogen and natural gas [30,41,50,55].

Properties	Diesel	Hydrogen	Natural gas
Main component	$C_{12}H_{23}$	H_2	Methane (CH_4)
Auto-ignition temperature (K)	553	858	923
Lower heating value (MJ/kg)	42.5	119.93	50
Density (kg/m^3)	833–881	0.08	0.862
Molecular weight (g/mol)	170	2.016	16.043
Flammability limits in air (vol%) (LFL–UFL)	0.7–5	4–75	5–15
Flame velocity (m/s)	0.3	2.65–3.25	0.45
Specific gravity	0.83	0.091	0.55
Boiling point (K)	453–653	20.2	111.5
Cetane number	40–60	–	–
Octane number	30	130	120
CO_2 emissions (%)	13.4	0	9.5
Diffusivity in air (cm^2/s)	–	0.61	0.16
Min ignition energy (mJ)	–	0.02	0.28

Table 4
In-cylinder peak pressure and temperature comparison for natural gas and hydrogen in various configurations [14,39,56–59].

Mode	Max pressure (MPa)		Max temperature (K)	
	HCCI	*CI*	*HCCI*	*CI*
H_2	~8	~12	–	–
NG	~7	~7.5	~1300	~1850
Diesel	~6.1	~6.6	–	~2300
NG+diesel	~3	~5.5	~1450	–
H_2+diesel	~7	~7.8	–	–

Table 5
Maximum BTE for hydrogen–diesel fuel compared with hydrogen HCCI, direct injection (DI) diesel and dual fuel [57,60].

	Diesel DI	Dual fuel (H_2+diesel)	H_2+diesel PPCCI	H2 HCCI	H2 DI
BTE (%)	27.9	33.9	36.5	45.0	42.8

2.4. Peak pressure and temperature

The variations of heat release rate during combustion affect the in-cylinder peak pressure and temperature. All these quantities (heat release rate, temperature and pressure) depend on the speed of the engine, equivalence ratio, load, intake pressure, temperature and energy content of the fuel configurations. Higher loads and richer mixtures typically produce higher peak pressures. Table 4 shows how the in-cylinder peak pressure and temperature vary for HCCI and conventional CI modes. These are general data to illustrate which mode produces a higher peak pressure. The data for maximum temperature is not fully reported but in general, temperature increases with pressure. HCCI configurations produce lower peak pressure than the conventional CI modes for every fuel configuration, leading to significant impacts on emission levels. Hydrogen addition to diesel influences the peak pressure generation. The higher the addition, the higher the peak pressure, and the addition of hydrogen is able to reduce ignition delay as well [40]. It can be concluded that the hydrogen fuel configuration yields the highest peak pressure and therefore produces better power and efficiency.

2.5. Brake thermal efficiency

The brake thermal efficiency (BTE) of an engine is the ratio of brake output power to input power and describes the brake power produced by an engine with respect to the energy supplied by the fuel. A study has been performed [14] to determine the best BTE for biogas fuels with an energy ratio ranges from 40% to 57% of biogas and an intake temperature of 80 °C, 100 °C and 135 °C. The biogas′ main component was methane (>60%), which was produced by anaerobic fermentation of cellulose biomass materials [29]. It was reported that the best energy ratio with diesel in HCCI mode was 51% biogas and the optimum efficiency occurred when the intake temperature was 135 °C. High energy ratios lower the heat release rate and the efficiency [14]. However, even when operated at the optimum biogas energy ratio, the BTE was no better than diesel running in CI mode. Duc and Wattanavichien [29] reported that biogas-diesel running in dual-fuel non-HCCI engines has a lower efficiency than diesel single fuel in either HCCI or non-HCCI mode.

Hydrogen, on the other hand, had a higher BTE than pure diesel in non-HCCI mode, increasing the BTE by 13–16% [30]. Szwaja and Grab-Rogalinski [40] reported that the BTE was increased from 30.3% to 32% with an addition of 5% hydrogen. The increase of BTE in hydrogen–diesel mode might be due to the uniformity of mixing of hydrogen

with air [41]. Hydrogen as a single fuel running in HCCI mode gives a BTE of up to 45% [39], showing that hydrogen is able to operate with extremely lean mixtures and still maintain a relatively high efficiency compared to diesel engines. Table 5 shows that hydrogen in HCCI mode yields better results compared to the conventional mode (45% vs. 42.8%) and hydrogen with diesel in non-HCCI mode produces a higher efficiency than diesel alone [57]. Therefore, it is expected that the combination of hydrogen and diesel in HCCI mode will produce a higher BTE than diesel in CI mode. This conclusion was reached with partially premixed charge compression ignition (PPCCI) configurations when reformed exhaust gas recirculation (REGR) was used with hydrogen-rich gas (no more than 24%) added to the intake manifold [60]. Some researchers use PPCCI instead of HCCI as they differ in their injection methods and both of them have the same purpose: to achieve a homogeneous mixture.

2.6. Exhaust gas emissions

Emissions levels have become a major focus in new engine developments nowadays because regulatory bodies, such as those in Europe, the United States (US) and Japan, are imposing stringent vehicle emissions quality standards [61–63]. Emissions in HCCI engines consist of UHC, CO, NO_x, and particulates. HCCI engines claimed to have low emissions levels on NO_x and particulate matters [14] and high levels of unburned hydrocarbons (HC) and carbon monoxide (CO) [14,64]. However, the emissions levels of an engine varies from one engine to another and is dependent on the operating conditions of the engine, fuel quality and the engine design [65,66]. Thus, the emissions levels from different engines cannot be directly compared with another engine because of those factors.

2.6.1. UHC, CO and CO_2

UHC and CO emissions in HCCI engines are higher than the conventional diesel engines as reported in [6,67,68] and are two of the challenges that need to be resolved. UHC is the consequence of incomplete combustion caused by low combustion temperatures [15,69,70] which cause deposition of fuel in boundary layers and crevices [58]. The level of UHC is generally specified in total hydrocarbon concentration, which is expressed in parts per million carbon atoms [71]. The source of UHC is reported from the crevice region, cylinder wall with thin layer of oil left when the piston moves down and any combustion wall which has a cold area [71,72]. Higher concentrations of hydrogen and natural gas in diesel engines have the ability to reduce UHC and CO emission levels, because the gaseous state of hydrogen and natural gas will reduce the wall wetting effect on the cylinder liner [73].

The amount of CO_2 and CO is dependent on the combustion efficiency, where the combustion efficiency can be defined as the ratio of CO_2 to the total of fuel carbon present in the exhaust including CO, CO_2 and UHC [74]. CO emissions are controlled primarily by the fuel–air equivalence ratio [71,75]. The principal reaction mechanism of CO formation is $RH \rightarrow R \rightarrow RO_2 \rightarrow RCHO \rightarrow RCO \rightarrow CO$, where R is the hydrocarbon radical [71]. The CO oxidation is dominated by the reactions of CO with OH radicals as $CO + OH \Rightarrow CO_2 + H$, which also forms hydrogen radicals. The conversion of CO to CO_2 occurs when the concentration of OH radicals increases during combustion [76]. For the HCCI engine with a low combustion temperature, the OH level is reduced resulting in an incomplete oxidation of CO [77]. The low combustion temperature will reduce the combustion efficiency as a result of the lower oxidation activity of the hydrocarbons and the lower conversion rate of CO to CO_2 [78]. Results of simulations confirm that the piston–ring crevice needs to be resolved in order to accurately predict UHC and CO emissions [6]. UHC and CO emissions originate in the crevices and boundary layer, which are too cold for complete consumption [79].

2.6.2. NO_x and particulate matter (PM)

The NO_x formation is explained by several formation mechanisms: Zel′dovich mechanism, Fenimore mechanism, fuel-bound NO_x, NO_2 mechanism and N_2O mechanism. In the Zel′dovich mechanism, also known as thermal NO_x, the NO_x is not formed from the fuel because there is no nitrogen component in the fuel. NO_x is formed in a high temperature reaction, where the nitrogen in air dissociates into nitrogen radicals to form NO when reacting with oxygen. Some NO is converted to NO_2 when further reactions occur in the chamber. The thermal NO_x is not significant when the combustion temperature is below 1800 K [76].

Under the Fenimore mechanism, also known as prompt NO_x, the NO_x is promptly formed in laminar premixed flames long before the NO_x is formed by the thermal mechanism. The Fenimore mechanism explains the additional NO_x produced over the Zel′dovich mechanism in hydrocarbon flames. Prompt NO_x is important for hydrocarbon fuels in fuel-rich conditions, where NO_x is formed by rapid reactions of hydrocarbon radicals (CH, CH_2, C_2, C_2H and C) with molecular nitrogen. Miller and Bowman [80] reported that NO_x formed by thermal mechanism is the dominant source of NO_x only in the equivalence ratio range of $\varnothing = 0.8-1.0$. For fuel–air equivalence ratio, $\varnothing < 0.8$, the temperature is sufficiently low and NO_x was formed by Fenimore mechanism.

The fuel-bound NO_x mechanism is used for coal and coal-derived fuels, where nitrogen exists as chemically bound to the major fuel. The NO_x formation is dependent on the local combustion temperature, stoichiometric conditions and the level of the nitrogen compounds in the fuel–air mixture. The NO_2 mechanism on the other hand, is based on the chemical kinetic calculations near the flame zone, where NO_2 is formed due to the reaction between NO and HO_2. The NO_2 then reacts with H and O radicals to form NO_x. The N_2O mechanism is also based on the chemical kinetic calculations, where the N_2O is formed due to the reactions of various nitrogen radicals with NO. The N_2O will finally react with oxygen radicals to form NO_x. In short, the NO_x formation is still under investigation and one cannot claim that all routes have been found [76].

Generally, most parts of the NO_x formation are determined by the peak temperature during combustion, where the peak temperature is dependent on other parameters as well such as equivalence ratio, fuel composition and the initial temperature of the fuel–air mixture [76]. Tanaka et al. [81] also reported that the NO_x levels are increased substantially when the equivalence ratio is more than 0.33. A higher equivalence ratio causes the maximum in-cylinder temperature to exceed 1800 K and produce more NO_x. In HCCI engines, the NO_x and particulate matters (PM) are reported to be very low [72,82] by implementing high CR engines. NO_x can also be reduced using high EGR rates by reducing the local temperature and decreasing the oxygen amount in the cylinder [70]. However, unburned HC and CO emissions will increase due to insufficient oxygen. Bression et al. [70] implemented a high-pressure-loop EGR without cooler and Variable Valve Timing (VVT) to reduce the NO_x, unburned HC and CO by increasing the combustion temperature. They reported that internal EGR by using VVT is an effective way to reduce the NO_x instead of using high-pressure EGR.

Papagiannakis and Hountalas [23] investigated the combustion and exhaust emission characteristics of a CI engine fueled with a blend of diesel (direct injected) and natural gas (port injected). They found that the NO_x level for dual fuel engine operation is lower than diesel CI engine. The NO_x can also be reduced by using hydrogen addition discussed in Section 5.3. The concentration of NO_x between natural gas and hydrogen in diesel HCCI mode is different due to different combustion temperatures, because hydrogen has a higher temperature and flame speed compared to natural gas and diesel [83]. A survey of research papers by

Akansu et al. [84] shows that the NO_x level is increased when the hydrogen content in natural gas–hydrogen mixtures is increased. It shows that the combustion temperature and the flame speed of hydrogen contribute to a higher level of NO_x emissions.

In biogas–diesel HCCI engines, the NO_x level was low when the biogas energy was increased [14]. This might be due to a higher homogeneity level achieved between air and fuels. Van Blarigan [85] in his study reported that the mixture must be homogeneous and lean in order to eliminate the production of NO_x. Olsson et al. [36] stated that the NO_x level is low in natural gas HCCI engines and when combined with exhaust gas recirculation (EGR), it drops further [15]. Even in natural gas–diesel non-HCCI mode, the NO_x level is lower than diesel conventional CI engines [86]. Hydrogen on the other hand produces zero UHC, CO and CO_2, due to the absence of carbon in the fuel, but still produces NO_x [50]. Hydrogen operated as a single fuel in CI mode yielded lower NO_x levels than diesel [57]. Saravanan and Nagarajan [30] in their study of hydrogen addition to diesel in non-HCCI mode showed that lower NO_x emissions were obtained for all load ranges compared to diesel in conventional mode. They reported that the formation of NO_x depends on temperature more than the availability of oxygen. Therefore, hydrogen–diesel in HCCI mode results in extremely low NO_x emissions levels with no significant amount of PM [87].

Kayes and Hochgreb [88] developed a mechanism model for PM and they reported that PM is produced due to liquid fuel nucleation from port fuel injection. The PM can also be produced from gas-phase nucleation in fuel-rich conditions. The air-to-fuel ratio strongly affects PM and burning liquid fuel will increase the amount of PM in the exhaust gas emissions [89], hence the use of a high pressure injection is advisable so that the fuel is in an atomized condition. PM can be reduced significantly when hydrogen is added to a diesel fueled engine [49] and also by heating the inlet [88]. When the engine runs in a dual fuel mode between diesel and natural gas, no significant reduction in PM was reported [90]. Hydrogen addition, on the other hand, shows a good advantage in reducing the PM emission levels.

2.7. Brake mean effective pressure

The brake mean effective pressure (BMEP) is an effective comparison tool to measure engine performance and indicates an engine's capacity to produce power output over the full engine speed range. It is also used to compare one engine's performance with another. A high BMEP shows the ability of the engine to perform high load operations. One of the HCCI engine's challenges is its limited load range because high load operations tend to produce knock [51]. Table 6 shows the BMEP ranges of standard engines. In comparison, the BMEP range for passenger cars (Saab 5 cylinders engine) operating in HCCI mode is only between 0 and 0.36 MPa [91], which is lower than the conventional SI engines.

Table 6
BMEP range for various engines types [71].

Engine type	Compression ratio	BMEP range (MPa)
SI engines		
Small (motorcycles)	6–11	0.4–1
Passenger cars	8–10	0.7–1
Trucks	7–9	0.65–0.7
Large gas engines	8–12	0.68–1.2
Diesel engines		
Passenger cars	17–23	0.5–0.75
Trucks	16–22	0.6–0.9
Large trucks	14–20	1.2–1.8
Locomotive	12–18	0.7–2.3
Marine engines	10–12	0.9–1.7

Natural gas–diesel in HCCI mode operates in the BMEP range of 0.25–0.4 MPa [14], which is low compared with the engines in Table 6. To increase the BMEP, the concentration of natural gas has been increased but if its concentration compared to diesel is too high, this will lead to knocking [14]. Fig. 2 shows that the best energy ratio for natural gas–diesel HCCI mode is about 51% and within the shaded region. For this optimized energy ratio, the maximum BMEP is only 0.4 MPa, which is a very limited load range and is not suitable for high load engine operations.

Hydrogen with diesel in HCCI mode is stable up to 0.6 MPa BMEP [60,87]. If a supercharger is used in hydrogen–diesel dual-fuel mode on a non-HCCI engine, a maximum BMEP of 0.91 MPa was reported [92]. Therefore, hydrogen and diesel in HCCI mode might be able to be used for high load engine operations.

2.8. Knocking

Knocking in SI engines is a phenomenon where the unburned mixture in the compressed gas ignites before it is reached by the propagating flame front [93]. Knock is physically detected when the engine vibrates excessively and a pinging sound can be heard outside as a result of the combustion activity. It causes loss of power and if not controlled, knocking could lead to severe engine damage and shorten its life. Knocking can occur in any reciprocating engine. HCCI engines are prone to knock since they are controlled by chemical kinetics and there is no fixed mechanism to control knock in them. Knocking phenomena limits the load range of an HCCI engine: high load operations can easily initiate knock, so upper load limits have to be applied [15]. In all engines, knocking occurs when the combustion starts before the piston reaches TDC, while misfire is when combustion commences after TDC. Knocking and misfire are two different behaviors which must be avoided in engine operation as both of them can contribute to deterioration of engine performance.

In natural gas–diesel HCCI engines, a misfire occurs when a high natural gas flow rate is combined with a low diesel flow rate while knocking starts with the opposite configuration [14]. If HCCI engines operate on hydrogen–diesel fuels, knocking is expected to occur when high amount of hydrogen is added. Knocking will take place if the hydrogen content is more than 16% of the energy ratio [40] which is confirmed by Guo et al. [94], who reported that it was necessary to use hydrogen with mass fraction less than 15% to achieve stable combustion. If an HCCI engine runs on natural gas with dimethyl ether (DME), the knock limit is at an in-cylinder pressure of 9 MPa and a very limited load range is obtained while getting unstable operation for high natural gas concentrations.

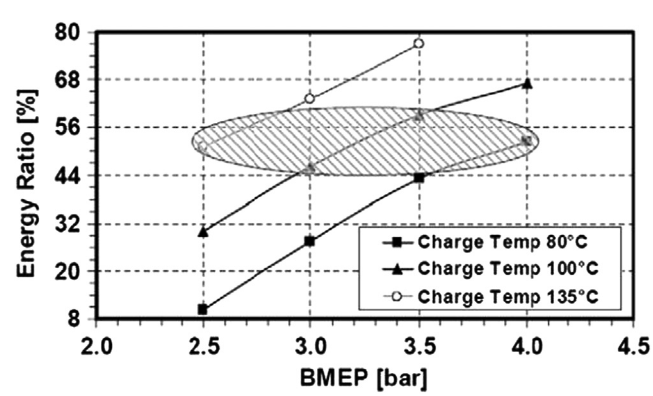


Fig. 2. BMEP for different intake temperatures with varying energy ratios between natural gas and diesel. The shaded region shows the best energy ratio for natural gas–diesel HCCI engines, reproduced from [14].

This was discovered by using Computational Fluid Dynamics (CFD) simulations with detailed chemical kinetics [51]. An investigation of auto-ignition and combustion of natural gas HCCI engines showed that knocking starts to happen when the equivalence ratio is less than 0.45 with an intake temperature of 380 K [16]. Fig. 3 shows the area of knocking and misfiring of natural gas HCCI engines with constant intake pressure. Thus, natural gas HCCI engines will not be able to operate at high load conditions due to this limitation.

Knocking occurs when a rapid release of energy in the remaining unburned mixture causes a rapid increase in local pressure. In hydrogen–diesel engines, the engine will not work in a stable condition if 100% hydrogen is used. A combination of hydrogen and diethyl ether (DEE) produces severe knock on 100% load [41]. As such, higher hydrogen content leads to a higher probability of knock onset. Knocking phenomena can be detected in the in-cylinder pressure variations, observing a rapid instantaneous local pressure rise. The graph formed depends on the knocking frequency: the higher the frequency, the more severe the knock [40]. Fig. 4 shows knocking behavior in a hydrogen HCCI engine for a single combustion event with a compression ratio of 17 by monitoring its in-cylinder pressure. It can be seen that the in-cylinder pressure suddenly increases to the peak before following the normal pressure trend: the peak pressure is higher than the normal in-cylinder peak pressure without knocking. The maximum increase in pressure for knocking is unpredictable and this abnormality usually occurs when there is an incorrect operating condition. Flowers et al. [26] have described the HCCI ignition by H_2O_2 decomposition. It accumulates due to low temperature reactions in the compression stroke. Once the in-cylinder temperature reaches 1050–1100 K, H_2O_2 decomposes rapidly into two OH radicals forming an enormous amount of OH radicals, which will rapidly consume the fuels. Reduction in OH concentration in low temperature regions leads to incomplete combustion, which delays the high-temperature oxidation [95]. However, there is no concrete mechanism in the literature describing the knocking phenomenon in HCCI engines and the methods to control it. In SI engines, it is quite easy to control knock. For example, car manufacturers usually install knock and oxygen sensors in the engine. If the mixture is prone to generate knocking, the sensors will automatically adjust the spark timing accordingly. However, in HCCI engines, there is no spark to control such situations and there is a strong dependence on the right mixtures and conditions.

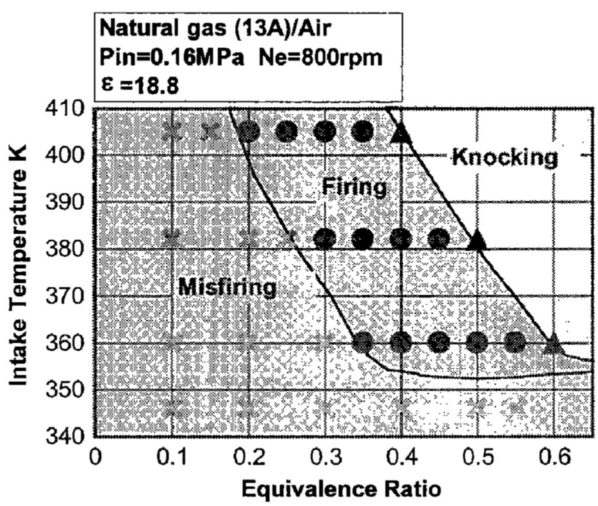


Fig. 3. Knocking and misfiring area for natural gas HCCI engines under constant intake pressure, reproduced from [16].

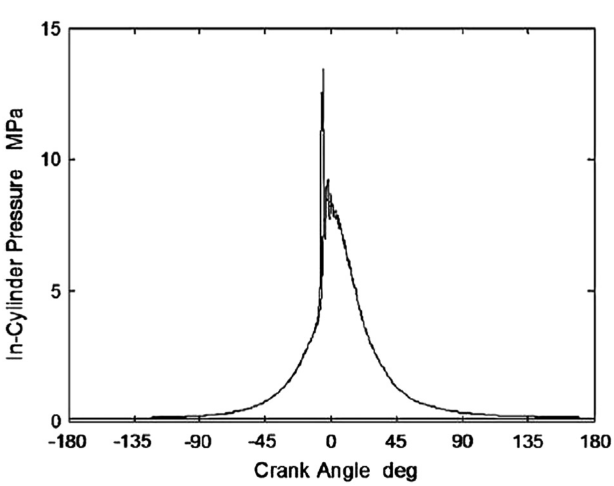


Fig. 4. Knocking phenomena in a hydrogen HCCI engine for a single combustion event, reproduced from [40].

3. Diesel injection methods for homogeneous mixtures

Vaporized diesel fuels are needed to initiate combustion in the conventional diesel CI engines, therefore a high diesel injection pressure is required. A higher injection pressure leads to better fuel vaporization and forms many small droplets of fuel leading to efficient fuel–air diffusion processes. Compression of air generates high in-cylinder temperatures, which is important to achieve the auto-ignition point of the diesel fuel. CI engines using common-rail injection systems employ injection pressures of at least 35 MPa to ensure the injected fuel is vaporized before the combustion takes place. However, in HCCI combustion using diesel, it is quite challenging to form a homogeneous fuel–air mixture before the initiation of combustion due to diesel's low volatility. Therefore, there are three methods to achieve homogenous mixtures in HCCI engines [21]:

1. Port injection.
2. Early injection.
3. Late injection.

3.1. Port injection

Port injection is the method of locating the diesel injector in the intake manifold, where the injection pressure is not as high as a direct injection system. Ganesh and Nagarajan [67] have studied the HCCI combustion of diesel with port injection, which they called "external mixture formation". It is used to form a homogeneous diesel–air mixture with injection pressures of no more than 0.6 MPa.

As the injection pressure is not high, the diesel fuel will not vaporize when entering the inlet manifold, creating undesirable inhomogeneity problem. To overcome this, the fuel vaporizer is to be mounted in the air intake manifold system so that the diesel is supplied in vapour form [67,69]. However, there are drawbacks when using port injection systems to form a homogeneous mixture: the soot is quite significant and NO_x is not as low as SI engines [21]. This might be due to the poor vaporization of the diesel, creating inhomogeneous mixtures. Another drawback is that the compression ratio has to be reduced to overcome knock, which leads to a reduction in engine efficiency. At the same time, it is difficult to control the start of combustion.

3.2. Early injection

Early injection uses the direct injection method, but with injection timing earlier in the compression stroke; there is no modification of the injection pressure from CI engines. Garcia et al. [58] have studied the performance of diesel engines operating in HCCI mode with early injection by varying the injection timing between 17° and 144° crank angle (CA) before top dead center (BTDC). It was found that CO and HC were higher in HCCI mode compared to the conventional CI mode due to fuel impingement on the cylinder walls [58]. Another study of the spray structure of common-rail type high-pressure injectors in HCCI engines obtained similar results [96]. The spray structure was simulated for early injection timing between 240° and 340° CA BTDC with an increment of 20° CA with injection pressures of 80 MPa and 100 MPa. It was found that if the fuel was injected earlier than 280° BTDC, the fuel would impinge on the cylinder wall and create a rich mixture, leading to incomplete combustion due to wall and crevice effects. However, if the fuel was injected at 300° CA BTDC, the fuel would impinge on the outer surface of the piston area. Any injection earlier than 320° CA BTDC, results in impingement on the piston bowl. This process is shown in Fig. 5.

It is obvious that early injection systems lead to fuel impingement problems on the cylinder wall and crevice areas. There are few methods to address this issue: using multiple injectors, multi-pulse fuel injection or narrow spray angle injectors. Multiple injectors will cause additional costs while multi-pulse fuel injection requires very precise control over injection timing by managing the injection pulse and its period [21]. Therefore it is hard to control the injection for different engine loads. Narrow spray angles might be an easier and cheaper way, which can be achieved by replacing the conventional injector (spray angle of about 156°) with a narrow spray angle injector (of about 60°). Kim and Lee [97] have studied the effect of narrow spray angle injectors in an HCCI diesel engine with an injection pressure of 100 MPa. They found that the narrow spray angle injector in HCCI engines using early injection timing is effective in maintaining a high IMEP [97]. The schematic diagram for narrow spray angle injectors is shown in Fig. 6. By using narrow spray angle injectors, the fuel will hit the piston bowl instead of the cylinder wall. However, the obvious drawback of using early injection is the difficulty in controlling the start of combustion. Therefore, one has to pay extra attention to the ignition delay effects.

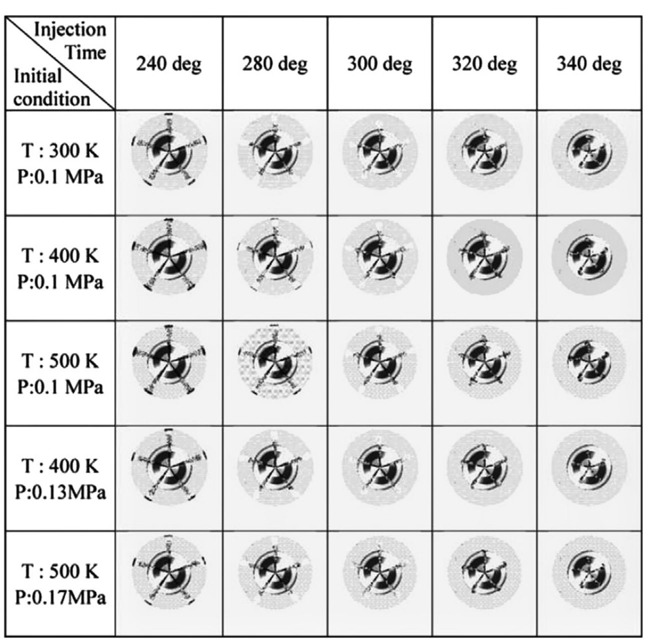


Fig. 5. Spray structure simulation result for various initial conditions, reproduced from [96]. The dark curved areas at the center represent the piston crown surface, the black circle line is the piston crown edges, the outer circle is the cylinder wall which in turn resembles piston edge and the five radial lines represent fuel being injected from the center. Spray structure behavior does not change much with initial conditions while it does with injection timing.

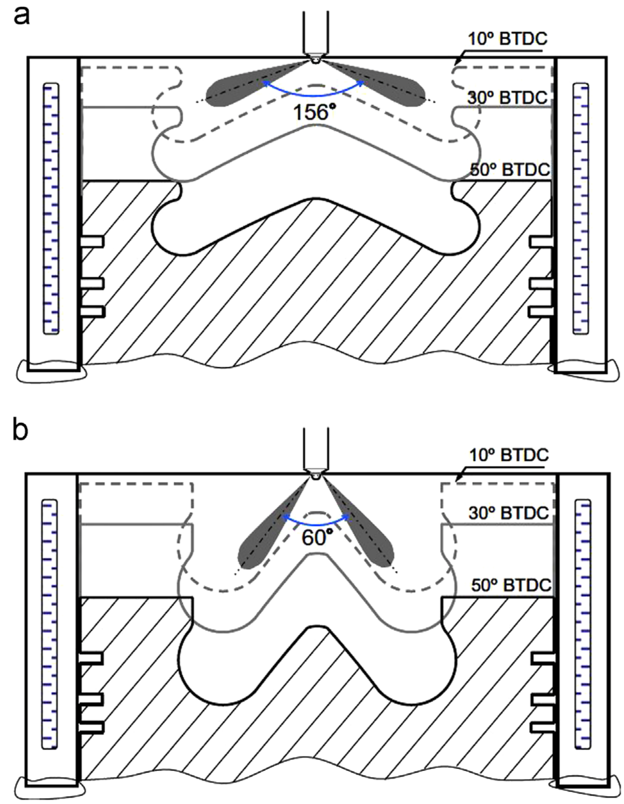


Fig. 6. Schematic diagram of the narrow spray angle injector, reproduced from [97].

3.3. Late injection

Late injection still uses a direct injection approach in order to minimize modification to the injection system. However, a high-injection pressure system is used with retarded injection timing at the end of the compression stroke or at the early power stroke. Conventional diesel ignition timing varies from 23° BTDC to 5° after top dead center (ATDC) depending on the equivalence ratio [98]. For late injection systems, typically the ignition timing is retarded up to 7° ATDC [21]. Late injection systems require a long ignition delay and rapid mixing rate [21,67]. The former can be achieved by implementing EGR (as discussed in Section 4.4), while the latter is dependent on the geometry of the combustion chamber. The Nissan Motor Company has developed a successful late injection system for HCCI engines by using Modulated Kinetics (MK) combustion systems [21]. They implemented high swirl effects in a toroidal combustion-bowl to achieve rapid mixing with a bigger piston bowl diameter. A higher piston bowl diameter is better as it can minimize the potential of fuel impingement on the piston bowl and the cylinder walls; Fig. 7 shows an overview of a piston bowl with toroidal geometry. This late injection system is able to control the start of combustion better than the first two methods.

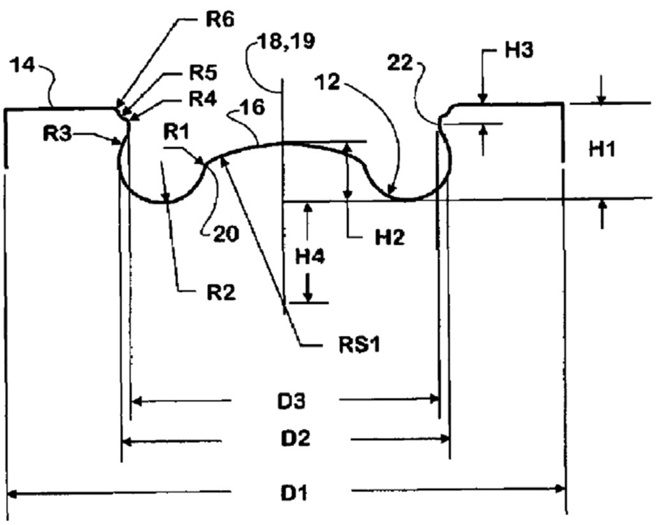


Fig. 7. Piston bowl with toroidal geometry, reproduced from [99].

4. Ignition control in HCCI engines

Ignition control is one of the challenges in developing HCCI engines. The challenges include [6,62]: (1) auto-ignition control; (2) limiting the heat release rate at high load operations; (3) meeting emissions standards; (4) providing smooth engine operation by achieving cold starts ('startability' of the engine); and (5) limited load range. Various studies have suggested that ignition can be controlled by using promoters or additives, blending of low cetane number fuels with high cetane number fuels [100], pre-heating of the intake air [15], pressurizing the intake air [101], hydrogen addition and varying the amount of exhaust gas recirculation (EGR) [26] through early closure of the exhaust valve.

Managing the ignition delay is one of the effective ways to control the start of combustion. Ignition delay is the time lag between the start of injection and the start of combustion. This is difficult to control because the combustion in HCCI engines is fully controlled by chemical kinetics. Too short an ignition delay leads to knocking while too long an ignition delay leads to misfiring. The ignition delay is strongly dependent on the gas temperature: an increase in temperature accelerates the chemical reactions, thereby helping to reduce the ignition delay [57,102]. Tanaka et al. [103] studied two-stage ignition in HCCI combustion, suggesting that the ignition delay can be controlled by the fuel–air ratio, initial temperature and additive dosages.

4.1. Pre-heat intake air

As discussed in the previous section (in Section 2.2), using natural gas and hydrogen in HCCI require a high intake temperature. By pre-heating the intake air, ignition delay is reduced and thus the ignition timing can be controlled. As shown in Fig. 1, methane and natural gas require high temperatures to auto-ignite and methane did not ignite for an intake temperature of 400 K at low CR [100]. Therefore, it is imperative to pre-heat the intake air to make the fuels combust smoothly.

Antunes, Mikalsen and Roskilly [39] stated that heating the inlet air is the most useful method to control the ignition timing. Questions may arise regarding the practicality of including electric heaters [16] in an engine bay just for this purpose: the heater causes the operation and maintenance costs to increase and contributes to extra engine weight. Installing a heater is an option used by most researchers as it is the easiest way to get intake air heated to some specific temperature. Exhaust gas recirculation (EGR) could be another option to reduce the need for a high intake temperature [15,43,69].

4.2. Pressurized intake air

Turbochargers and superchargers are commonly used in real engine applications because they can be applied to any internal combustion engine. The operational concepts of these two devices are the same: to provide a high intake pressure into the combustion chamber, increase the charge density and thereby increase the engine performance. Some studies [101,104,105] show that the start of combustion (SOC) is advanced if the intake pressure is increased by 0.1 MPa. This indicates that pressurized intake air is able to improve the auto-ignition of the fuel. However, these situations also depend on the type of fuel used, and in this case they used primary reference fuels and gasoline. By increasing the intake pressure, it was possible to get the auto-ignition to start at 15° before top dead center (BTDC). On the other hand, supercharging (pressurizing intake air) is able to increase engine efficiency [7]. A supercharged hydrogen–diesel engine, but in non-HCCI mode, was able to maintain high thermal efficiencies and it was possible to use more than 90% hydrogen energy substitution for the diesel [60]. Another study by Guo et al. [94] shows that hydrogen–diesel in HCCI mode with pressurized intake air (150 kPa) is able to improve the atomization process, and therefore improve the combustion efficiency. CO, HC and NO_x emissions were also decreased in this case.

4.3. Hydrogen addition

Hydrogen is one of the promising renewable fuels because it is naturally available on the earth and can be produced from various resources such as fossil energy and biomass [106,107]. Hydrogen can be used as a sole fuel in an SI engine but cannot be used in a CI engine due to its higher ignition point compared to diesel [108,109]. The used of hydrogen in internal combustion engines requires extra care due to safety reasons. According to Najjar [106], there are three hazards associated with the use of hydrogen, which are physiological (frostbite and suffocation), physical effect (embrittlement and component failures) and chemical (burning or explosion). Proper hydrogen installation such as high pressure vessel is required to avoid physiological effect. The ability of hydrogen to permeate through steel may cause an embrittlement effect and lead to component failures. Fayaz et al. [110] reported that to avoid the embrittlement effect on some metals, the following alloys can be used in a hydrogen engine application: brass and copper alloys, aluminum and its alloys and copper beryllium. The crank case design of the engine should also be taken into consideration so that it has good ventilation. The blow-by effect causes unburned hydrogen to enter the crankcase and at certain concentrations may lead to combustion. The hydrogen injection method also plays an important role in avoiding undesired explosions. Direct injection is a preferred method over port injection to avoid the backfire effect [110]. Backfire is combustion occurring during the intake stroke due to hot spots and could also occur in the intake manifold [50]. It is of the utmost importance to avoid any undesired combustion behavior for safety reasons.

Hydrogen can be produced in many ways including natural gas conversion, coal gasification, electrolysis, biomass gasification and photolytic processes [110]. However, the conversion cost of hydrogen using current technology is still very expensive [106] and it is not practical to have a separate hydrogen vessel for a vehicle with dual fuel technology because the combined fuel cost becomes higher. Thus, an on-board hydrogen generator is a possible solution to overcome this high hydrogen conversion cost and also the problems associated with storage and handling [111]. Tsolakis and

Megaritis [87] used a fuel reforming reactor in the diesel exhaust system to extract hydrogen. Bromberg [112] used a plasmatron fuel converter to convert a gas containing hydrogen, while Bari and Esmaeil [113] used water electrolysis to generate hydrogen.

Hydrogen addition in a CI engine is able to reduce UHC, CO and smoke emissions, however, NO_x emission is increased due to the high combustion temperature [49,107,109–111,114,115]. To reduce the NO_x, intake charge dilution with nitrogen can be used [111], or EGR [110]. With nitrogen dilution, the NO_x level is reduced substantially, however, smoke, CO and fuel consumption are increased. EGR, on the other hand, causes increase in PM, UHC, CO and also engine wear. Thus, Miyamoto et al. [116] recommended using large amount of EGR and late diesel-fuel injection timing for diesel engine with hydrogen addition. They reported that the NO_x emission is low without the increase in UHC due to low combustion temperature.

Hydrogen addition to the HCCI engine is one of the effective ways to reduce the ignition delay due to its high diffusivity in air, which causes rapid mixing between fuels and oxidizers. Hydrogen addition in a natural gas mixture is able to increase the in-cylinder peak pressure, reduce ignition delay time and ignition temperature, and increase indicated power [1]. It also allows the extension of the lean limit of the natural gas mixture, without entering the lean misfire region, while achieving extremely low emissions [50].

Hydrogen addition in ultra-low sulfur diesel (ULSD) promotes partially-premixed compression ignition and results in improved performance and reduction in emissions [60]. In HCCI engines, hydrogen is able to form a homogeneous mixture due to its rapid mixing behavior, and thus increase the efficiency of the engine [41]. Furthermore, hydrogen can be produced from the exhaust gases of the engine itself using a reformer, which is called an "on-board hydrogen producer" [15,87]. As the amount of hydrogen is increased, the auto-ignition delay time reduces accordingly while as the in-cylinder peak pressure is increased, the ignition temperature reduces and indicated power increases [1]. The addition of hydrogen is not costly because it uses a lower-pressure fuel-injection system [79].

Furthermore, the addition of hydrogen increases the engine efficiency by a significant margin, about 13–20% [30,41]. By using a catalytic reforming aid in HCCI, the addition of hydrogen in natural gas HCCI engines helps in decreasing the need for high intake temperatures and also is a means of extending the lower limit of HCCI operations [43]. It can be seen from Fig. 8 that the in-cylinder peak temperature increases and the ignition delay time reduces as the amount of hydrogen increases.

Szwaja and Grab-Logarinski [40] studied hydrogen addition (in HCCI mode) with diesel in a CI engine and found that the addition of hydrogen in small amounts (e.g. about 5% in energy ratio) was able to reduce the ignition delay and improve engine performance. They also concluded that the addition of hydrogen to diesel should not be more than 15% in energy ratio to avoid severe knock.

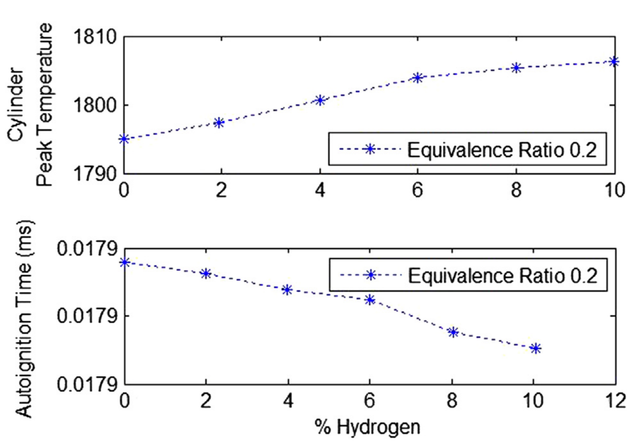


Fig. 8. Hydrogen effect on the in-cylinder peak temperature and the ignition delay [1].

4.4. Exhaust gas recirculation (EGR)

EGR is a system where some portions of the exhaust gas are returned to the combustion chamber, controlled by using a valve. Exhaust gas contains less oxygen (O_2) and more CO_2: combustion with reduced O_2 will lower the combustion temperature, and thus reducing the NO_x emissions. It is also used to reduce the large heat difference between peak pressure and intake pressure. This means that the intake temperature of using EGR is high and certainly helps in auto-ignition of the mixture. Saravanan and Nagarajan [30] reported that EGR is able to increase the BTE of the engine, while reducing the NO_x formation. Furthermore, EGR improved auto-ignition of the engine and reduced the in-cylinder peak pressure. EGR used in a diesel HCCI engine showed an improvement of 1.1% engine efficiency, advanced the auto-ignition by 10° and reduced the heat release rate by 11 J/deg CA compared to diesel fuel [69]. Ganesh and Nagarajan [67] found that by using EGR on diesel HCCI engines, they were able to reduce the heat release rate with a lower combustion temperature. They could control ignition delay as well as reduce the in-cylinder peak pressure. However, using EGR leads to a power loss of 20% when used with diesel fuels [58].

4.5. Addition of dimethyl ether (DME), hydrogen peroxide (H_2O_2), formaldehyde or n-butane

Additives do not seem to lead to any major practical improvements, due to the addition of extra chemical compounds, which leads to an increase in operational cost. However, with the help of additives, the start of combustion of DME in a natural gas/DME mixture is improved by reducing the ignition delay time. It was found that methane-fueled HCCI engines with an intake temperature of 400 K ignited only if small amounts of additives were added [100]. This shows the advantage of using additives, which can control the auto-ignition timing, but with extra drawbacks.

5. Numerical study of HCCI engines

Simulations are undertaken to reduce research costs while maintaining good productivity because of their cost efficiency compared to experimentation alone. By using numerical methods, one can optimize engine parameters before conducting experiments and obtain optimized parameters within a short time and low cost. Many researchers use KIVA-3V CFD software in combination with detailed chemical kinetics solutions using CHEMKIN from Sandia National Laboratories [104,117–120]. Good agreement between simulations and experiments has been achieved.

5.1. Chemical kinetics

In a CI engine, the fuel is direct-injected in the chamber with high injection pressure when the piston is nearly at TDC. Then, the fuel ignites rapidly in the hot air environment. In SI engines, the spark plug is triggered when the piston is approximately at TDC to initiate the combustion. HCCI engines, on the other hand, have no mechanism to control the ignition timing and rely solely on chemical kinetics for combustion, as discussed in Section 3. The combustion in an HCCI engine is triggered when the heat in the chamber has reached the fuel activation energy. To numerically investigate the combustion behavior, chemical kinetic mechanisms which represent the actual fuels have been developed [121–126]. A detailed mechanism such as those

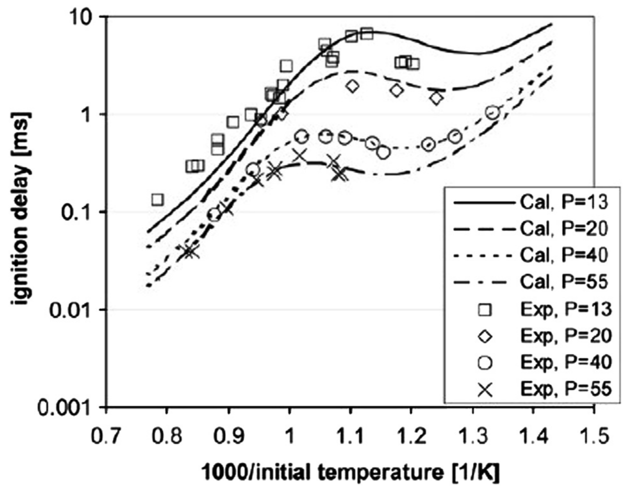


Fig. 9. Ignition delay time for *n*-heptane validated against experiment for different pressures [131].

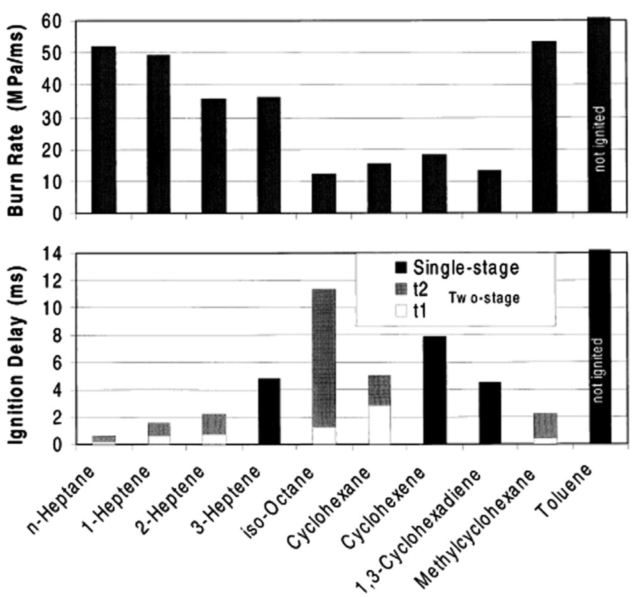


Fig. 10. Summary of ignition burn rate and delay time for different types of fuels [103].

developed for diesel fuel consists of a blend of components such as *n*-alkanes, *iso*-alkanes, *cyclo*-alkanes, aromatics and others [127]. Those components were then combined to represent the real fuels [128]. Most studies on developing the chemical kinetic mechanism [46,121,122,125,127,129] for HCCI engines use the Arrhenius-like plot (such as shown in Fig. 9) to relate the fuel activation energy with ignition delay time, where the activation energy is proportional to the slope of the graph [130].

Small variations in fuel properties affect the HCCI combustion by having a different ignition delay time. Fig. 10 shows the ignition delay time and burn rate of different fuels [103]. The *n*-heptane has the lowest ignition delay time, while *iso*-octane has the highest with a slower burn rate. This shows that the ignition delay time (for multiple ignition stages as in Fig. 10) and burn rates are dependent on the fuel structure. Tanaka et al. [103] reported that the failure on Toluene auto-ignition is due to the high activation energy required to abstract the hydrogen (H) radical from the carbon chain.

Westbrook et al. [127] studied the detailed chemical kinetic models for large *n*-alkanes, which can be used to represent the diesel fuel. The aim was to investigate the model that can use less computing resources by having an almost identical ignition behavior compared to the experiment. They found that the ignition delay time is not affected significantly for different carbon lengths. Thus, they concluded that a small *n*-alkane such as *n*-octane can be used as a surrogate fuel for diesel which has the same ignition behavior of a much larger *n*-alkane like *n*-hexadecane. Many studies have been conducted to develop a chemical kinetic mechanism that can represent the actual fuels. This is summarized in Table 7, where it shows different chemical kinetic mechanisms to represent different fuels.

It is common to use *n*-heptane as a surrogate fuel for diesel [132–135] because the chemical properties between those two are very similar in term of cetane number. The intake temperature when *n*-heptane is used as a fuel in a HCCI engine is not as high as methane or natural gas. A study by Guo et al. [132] showed that the *n*-heptane can be easily ignited when the inlet temperature is 313 K on a low CR engine (CR = 10). Methane, on the other hand, is reported to have no ignition when the inlet temperature is less than 400 K on a high CR engine (CR = 15) [31]. Thus, it is important to have the right fuel and its chemical kinetic mechanism in order to study the combustion behavior of an HCCI engine.

Curran et al. [121] developed a detailed mechanism for *n*-heptane and validated the result over a wide range of operating conditions. They found that the ignition delay is in very good agreement with experiments using flow reactors, shock tubes and rapid compression machines. Because a detailed mechanism uses more computational resources, Seiser et al. [136] and Golovitchev [123] developed a reduced mechanism for *n*-heptane. Patel [137] reduced the mechanism by more to obtain 26 species and 52 reactions. He reported that the CPU time is reduced by 50–70% and the validation was completed under both constant-volume reactor and HCCI engine conditions. The ignition delay result is similar to those of detailed mechanisms. The use of *n*-heptane as the only main component in the mechanism is not sufficient to predict the soot emission from CI and HCCI engines. Thus, Wang et al. [138] improved the mechanism by blending the *n*-heptane and toluene mechanisms. They reported that the mechanism gives reliable soot predictions and combustion phasing under various engine conditions.

An *iso*-octane mechanism was used as a surrogate fuel for gasoline and it can also be blended with *n*-heptane to represent a real fuel [81,122]. A real gasoline fuel consists of thousands of hydrocarbon compounds [139,140] and the fuel should have been modeled using a combination of a few components. Mehl et al. [125] developed a mechanism that represents a commercial grade gasoline, which consists of *n*-heptane, *iso*-octane, toluene and olefins. They reported that the result is in good agreement over a wide range of pressures and temperatures relevant to internal combustion engine applications. A reduced mechanism was also developed by Mehl and Chen et al. [141] and further reduced by Lee et al. [124]. A reduced mechanism shows an advantage when used in a complex CFD model, which requires more computational resources [124].

Natural gas mainly consists of methane as the main components, as shown in Tables 1 and 3. A mechanism for methane called Gri-Mech [142] has received wide attention, such as [31,100,143]. A further development of the methane mechanism has ended with the final version being Gri-Mech 3.0. Then, reduced mechanisms were developed based on the Gri-Mech mechanisms such as those from [144]. A recent development of the methane mechanism has been developed by Slavinskaya et al. [145]. The mechanism was validated for high- and low-pressure conditions for rocket applications. They take into consideration

Table 7
Chemical kinetic mechanisms available for different fuels.

Fuel	Main components	Year	Number of species/ number of reactions	Temperature range (K)	Pressure range (bar)	Equivalence ratio range
Diesel	*n*-Heptane	1998 [121]	565/2540	550–1700	1–42	0.3–1.5
	n-Heptane	2000 [136]	159/770	625–1667	1–13.5	–
	n-Heptane	2003 [123]	57/290	600–1300	6–42	0.5–3.0
	n-Heptane	2004 [137]	26/52	700–1100	40–50	0.2–1.0
	n-Heptane/toluene	2013 [138]	71/360	–	–	–
Gasoline	*Iso*-octane	2001 [139]	101/479	600–1400	10–40	0.22–2
	Iso-octane	2002 [122]	857/3606	550–1700	1–45	0.3–1.5
	Iso-octane	2002 [140]	45/69	–	–	0.2–0.7
	Iso-octane	2003 [81]	32/55	750–900	30–50	0.2–0.6
	n-Heptane/*iso*-octane/toluence	2003 [123]	119/621	600–1300	20–50	1
	n-Heptane/*iso*-octane/toluene/olefins	2011 [125]	1389/5935	650–1200	3–50	0.5–1.3
	n-Heptane/*iso*-octane/toluene/olefins	2011 [141]	312/2469	650–1200	3–50	0.5–1.3
	n-Heptane/*iso*-octane/toluene	2011 [124]	48/67	700–1200	40	0.5–2.0
Natural gas	Methane	1999 [142]	53/325	1000–2500	0.01–10	0.1–5
	Methane	2001 [151]	37/351	–	–	–
	Methane	2006 [152]	55/278	900–1400	16–40	1
	Methane	2007 [153]	19/15	1000–2000	1–30	0.5–1.5
	Methane	2012 [144]	14/9	300–1800	40–60	0.7–1
	Methane	2013 [145]	37/354	300–1800	0.02–100	0.5–3.0
Hydrogen	Hydrogen	1995 [146]	9/20	250–2500	0.05–87	0.2–6
	Hydrogen	2004 [154]	10/18	298–2700	0.05–87	0.2–6
	Hydrogen	2012 [155]	9/14	900–1400	1	0.5–5
	Hydrogen	2012 [147]	11/19	1000	1–30	0.5–4.5
Biofuels	Ethanol	1999 [156]	57/383	300–2500	1	0.5–2.0
	Methanol	2002 [157]	52/326	–	–	–
	Ethanol	2006 [158]	112/484	–	–	–
	Methyl butanoate	2007 [159]	295/1498	800–1350	1–13	0.35–1.5
	Methyl butanoate/*n*-heptane	2008 [160]	53/156	650–1350	40–60	0.4–1.5
	Methyl decanoate/methyl-5-decenoate/ methyl-9-decenoate/*n*-heptane	2010 [148]	3036/8555	800–1400	10	0.5
	Methyl decanoate/methyl-9-decenoate/ *n*-heptane	2012 [161]	115/460	700–1800	1–100	0.5–2
	Butanol	2012 [162]	426/2335	720–1700	0.04–80	0.6–1.7
	Methyl decanoate/methyl-9-decenoate/*n*-heptane	2013 [163]	69/192			

the depletion of ozone layer. The result shows that a methane–air propelled liquid rocket engine influences the formation of nitrogen compounds and thereby depleted the ozone.

Hydrogen mechanisms, on the other hand, show a matured development, where the species and reactions are not substantially varied. A well-developed hydrogen mechanism in 1995 by Marinov et al. [146] has been validated over a wide range of operating conditions, including high-pressure combustion. A recent development by Burke et al. [147] focused on the discrepancies (in reaction rate parameters) between experiment and simulation. They reported the characterization of the non-linear mixture for $H+O_2(M)=HO_2(+M)$ might be necessary to predict high pressure flame speed within an accuracy of 5%.

Biofuel is considered as an alternative fuel and is produced from long-chain fatty acids derived from either vegetable or animal oil. The trans-esterification method is used to transform these large molecules into esters, where methanol is commonly used during the trans-esterification process [148]. The focus of using biofuels has received increasing attention [47] because of the advantage as alternative fuels. Biofuel can be extracted from fats or vegetable oils [149] and also algae [150]. The chemical kinetics development for biofuels has advanced to the next level by blending the *n*-heptane and methyl esters to represent rapeseed and soybean derived biodiesels, such as those developed by Herbinet et al. [148]. They reported that the ignition delay is in good agreement with experiment using rapeseed oil. The mechanism can also be used for modeling the biofuel from various origins by adjusting the mole or mass fractions of the components (methyl decenoate, methyl-5-decenoate, methyl-9-decenoate and *n*-heptane) according to the actual biofuel blends. For more detail on chemical kinetic reaction mechanisms available for biofuels, one can refer to a review paper by Komninos and Rakopulous [47].

5.2. Numerical and CFD environments

Numerical modeling can be categorized by the number of dimensions considered: zero-dimensional, quasi-dimensional and multi-dimensional. CFD is a multi-dimensional method whereby it resolves very small-scale zones and typically produces a more accurate result. A zero-dimensional model is the simplest model where there is only one independent variable, typically either time or, equivalently, crank angle, and an empirical heat release model is normally applied. The advantage of zero-dimensional model is that the run time is fast (computationally effective) and therefore it can be utilized for immediate use of engine design and analysis. However, the disadvantage of this method is that the simulated combustion duration is shorter than the actual duration due to inhomogeneities in reality [21]. The calculated results of zero-dimensional models produce rapid

pressure increases and very high heat release rates compared to actual HCCI engine combustion [143]. A quasi-dimensional model uses a turbulent sub-model for turbulent combustion and to derive a heat release model. Fig. 11 shows three different interacting regions for a quasi-dimensional model which is typically used to improve upon the zero-dimensional model. However, UHC emissions are over-predicted by 5–15% and CO emissions exhibit a 50% error. This is due to the inability of the model to capture small temperature differences in the crevices [101,164].

5.3. Single-zone and multi-zone models

A single-zone model is where the combustion chamber area is treated as one homogeneous block. A multi-zone model separates the combustion chamber into several zones and the zone distribution depends on the type of the engine, either based upon flame propagation or homogeneous mixtures, thereby representing the inhomogeneity in the cylinder prior to combustion [21]. The zone distribution for HCCI engines is shown in Fig. 12(a) while Fig. 12 (b) is a multi-zone model for SI engines. Multi-zone modeling of HCCI engines is organized in such a way because the heat generated in an HCCI engine comes from the core of the combustion chamber. This is different to SI engines where the zone is started from the spark plug (the location of the heat source), and propagated according to the flame front motion.

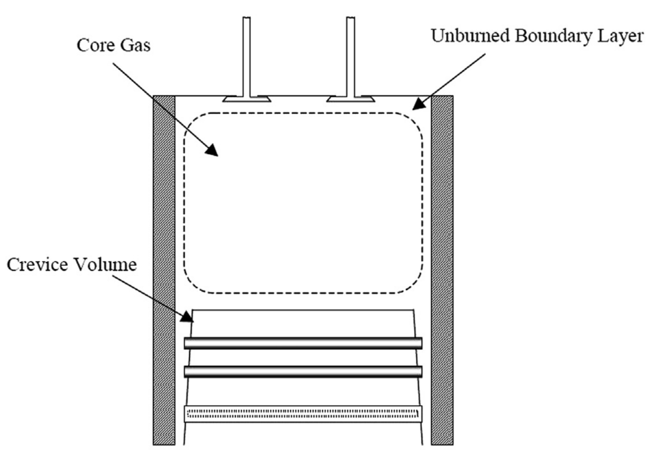


Fig. 11. General layout of the quasi-dimensional simulation showing the interacting adiabatic core, thermal boundary layer and crevice regions, reproduced from [101].

The single zone model has some limitations due to the assumption that the whole combustion chamber is treated as homogeneous. Peak cylinder pressure and rate of pressure rise can be over-predicted, as shown in Fig. 13(a). It also predicts a short burn duration and cannot accurately predict CO and HC emissions, which primarily depend on crevices [100]. Crevices and the boundary layer are the cold areas for HC and CO to react during combustion. On the other hand, the multi-zone model predicts the pressure trace and the peak cylinder pressure very well, as shown in Fig. 13(a), but it also cannot consider boundary layer effect and crevices, thus cannot predict CO and HC emissions [165]. Better agreement in combustion phasing is achieved when the single-zone model is coupled with detailed chemical kinetics and turbulent mixing effects [4], as shown in Fig. 11(b).

If there is any inhomogeneity in the mixture, turbulence has an effect on combustion, while for a completely homogeneous mixture, turbulent mixing has little effect on the combustion heat release rate. However, it is suspected that there will be inhomogeneities in the mixture as there is often insufficient time to mix down to the smallest relevant scales, which would cause turbulent

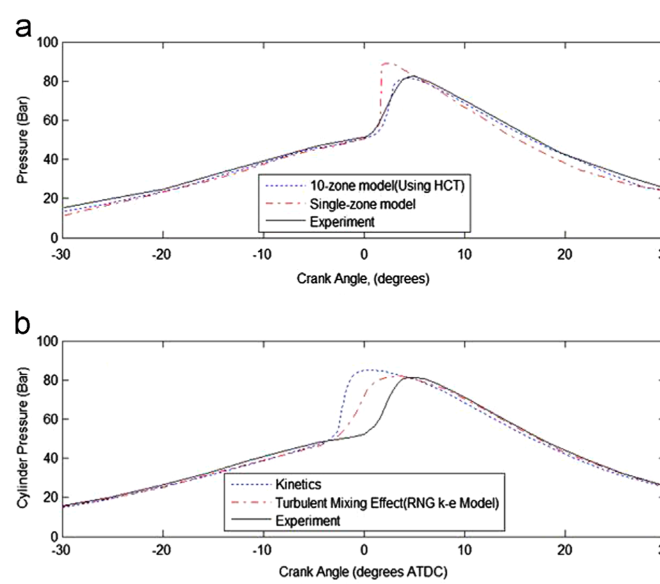


Fig. 13 (. a) Comparison between single-zone and multi-zone models with experiment [165]. (b) Comparison between experiments, single-zone model coupled with chemical kinetics only, and coupled with chemical kinetics and turbulent effects [4].

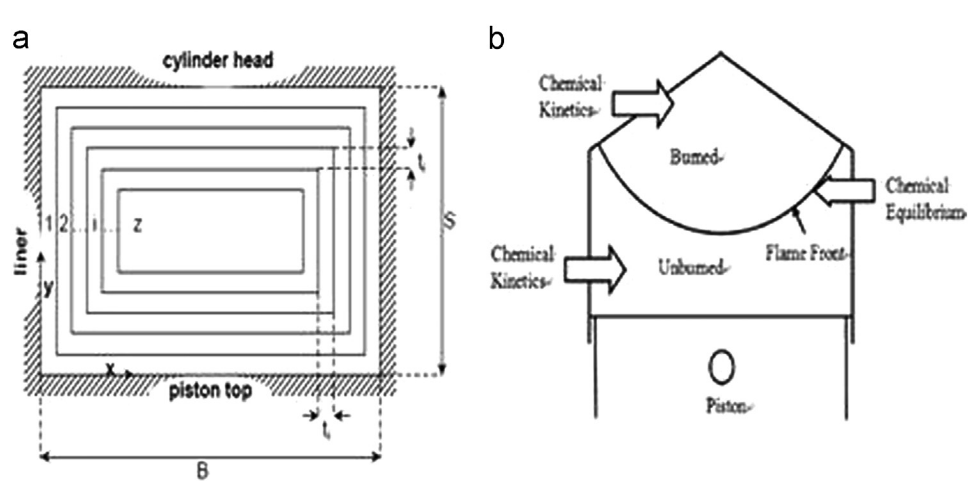


Fig. 12. Multi-zone model geometric configuration difference (a) HCCI engine, reproduced from [44] and (b) SI engines, reproduced from [166].

mixing to directly affect reaction rates [4,6]. In actual combustion chambers, transportation of chemical species, heat transfer and heterogeneity of temperature and species concentration exist [43]. A multi-zone model of HCCI combustion predicted maximum pressure, burn duration, indicated efficiency and combustion efficiency with the worst error of 10% [165]. However, UHC and CO emissions were under-predicted; Aceves et al. [165] suggested that this might be due to some crevices not being considered in the analysis. They used a multi-zone model including zones in crevice regions producing more accurate results.

5.4. Multi-dimensional models: CFD

A multi-dimensional model solves the equations for mass, momentum, energy and species conservation to obtain more accurate results at the expense of computational time and resources. When solving detailed chemical kinetics, a sequential operation is used to reduce computational time by solving the flow field then the chemistry rather than attempting to satisfy both simultaneously. Two common approaches to multi-dimensional modeling are multi-zone models and CFD. A multi-zone model requires substantially less computational time and resources than CFD at the expense of accuracy. However, Aceves et al. [167] showed that a 40-zone model can successfully predict the effect of crevice geometry on HCCI combustion with combustion efficiency predicted within 5% error compared to experiment.

A study has been performed using two-step processes in CFD to analyze combustion [10]. First, KIVA CFD was used for the effect of turbulence to solve the transport of all variables. Then the result from KIVA was used in the hydrodynamics, chemistry and transport (HCT) code to calculate the combustion parameters. This two-step method made it possible to obtain accurate predictions for turbulent combustion within a reasonable computational time [10]. The proposed approach using the CFD method can provide an accurate prediction of the combustion process and accounts for mixture inhomogeneities in both temperature and composition [168].

5.5. Effect of operating parameters on ignition delay time

As discussed in Section 4, the ignition in HCCI engines can be controlled using a number of parameters. This can also be discussed using a numerical approach, where the chemical kinetics was used to investigate the ignition delay time for different fuels. Tanaka et al. [81] developed a reduced chemical kinetic model for a primary reference fuel (PRF), which is a blend

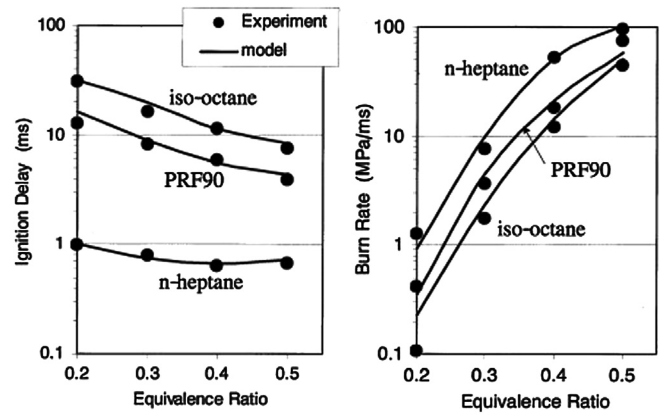


Fig. 15. The effect of equivalence ratio on the ignition delay and burn rate for *n*-heptane, *iso*-octane and primary reference fuel (PRF) [81].

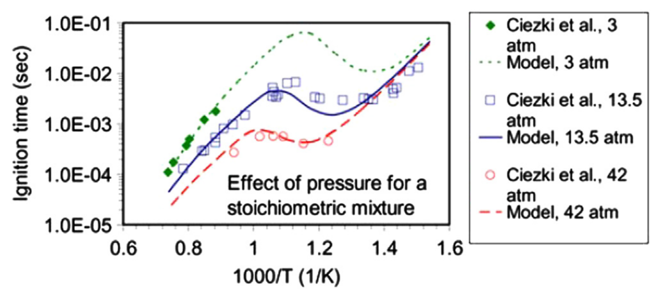


Fig. 16. The effect of different pressures on the auto-ignition delay time for a stoichiometric mixture of *n*-heptane/air [170].

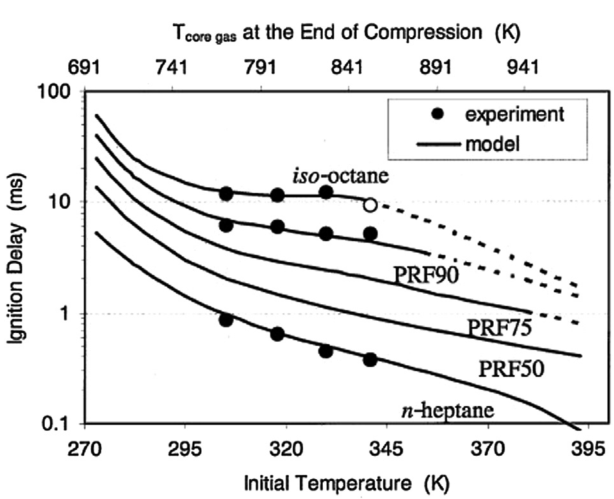


Fig. 14. The effect of initial temperature on ignition delay time for different fuels [81].

of *n*-heptane and *iso*-octane. They validated the model in a rapid compression machine (RCM) to represent HCCI combustion. The comparison was made between *iso*-octane, PRFs and *n*-heptane. The results in Figs. 14 and 15 show the ignition delay time for the selected fuel mechanisms with varying initial temperature and equivalence ratio. The results indicate that *n*-heptane has the fastest ignition delay time compared to PRFs and *iso*-octane. When the inlet temperature increases, the ignition delay time reduces further, where all fuels follow the same trend, as expected. The ignition delay time is also decreased when the equivalence ratio is increased towards the rich mixture, where the *n*-heptane has the fastest ignition delay time irrespective of the equivalence ratio compared to other fuels, as shown in Fig. 15. The *n*-heptane also has the highest burn rate, which shows its characteristic of susceptibility to auto-ignite.

The results of ignition delay time between *n*-heptane and *iso*-octane by Tanaka et al. [81] is consistent with experiment. As discussed in Section 5.1, the *n*-heptane can easily be ignited using an inlet temperature of 313 K on a low CR engine. Gasoline, on the other hand, requires an inlet temperature of 453 K to auto-ignite for a high CR engine (CR = 14.5) [169]. This shows that gasoline needs higher chemical activation energy compared with *n*-heptane. Different fuels require different inlet temperature to auto-ignite, as shown in Fig. 1, due to different ignition delay times. The inlet temperature requirement reduces as the compression ratio of the engine increases. This is also consistent with Olsson et al. [36], where they studied the effect of compression ratio on a natural gas fueled HCCI engine. They found that as the compression ratio increased, the required inlet temperature decreased, which reduced the ignition delay time.

The effect of different inlet pressure using chemical kinetics is investigated by Puduppakkam et al. [170]. They studied the

ignition delay time between diesel and gasoline using detailed chemical reaction mechanisms. The *n*-heptane mechanism used as a surrogate fuel for diesel consists of 3809 species and 15,678 reactions. The surrogate fuel for gasoline consists of 1833 species and 8764 reactions. Both surrogate fuels use a blend of several chemical classes, such as normal-, *cyclo*- and *iso*-alkanes, alkenes and aromatics. The result is shown in Fig. 16 for *n*-heptane, where the ignition delay time reduced as the inlet pressure increased. The pressurized intake air is able to increase the charge density and engine performance, and also can be used as an effective tool to control the ignition in HCCI engines, as discussed in Section 5.2.

Fig. 17 shows the effect on ignition delay time when EGR is employed. It shows that the ignition delay time is slightly increased when EGR increases (reduction in O_2 mole fraction). The result in Fig. 17 also shows that the ignition delay time reduces when the inlet pressure increases. The effect of EGR is also discussed by Christensen and Johansson [3], where they studied the mixture quality using *iso*-octane, ethanol and commercial-grade natural gas in a high CR HCCI engine. They reported that the ignition delay time also increased when EGR was used. This in return gives retarded combustion and slows the combustion rate, which is useful to reduce the combustion noise and also knocking.

Knocking, as discussed in Section 2.8, is due to the instability in combustion phasing. Unstable combustion may cause knocking or misfiring (advanced or retarded ignition timing). EGR is able to retard the ignition timing and also to obtain higher loads, but too much retarded combustion causes misfiring especially for the fuel with longer burn duration [171]. The combustion phasing in HCCI engines is difficult to control at high loads because the stability limits between knocking and misfiring is narrow [172]. Maurya and Agarwal [173] reported that the unstable combustion is due to high cycle-to-cycle variation and to overcome this, they used closed loop control to monitor the combustion phasing.

Olsson et al. [36] in their study of compression ratio influence on the maximum load of a HCCI engine reported that the combustion-phasing stability is due to the coupling between chemical kinetics and thermal problems. The gas temperature during combustion is influenced by the wall temperature or heat transfer rate, which affects the ignition timing. The instability in combustion becomes more severe at high loads, where the unstable combustion causes advanced or retarded combustion, as shown in Fig. 18. They employed hydrogen addition to control the ignition timing. The mass fraction of hydrogen was increased in order to advance the ignition. Once the wall temperature was substantially increased, the hydrogen amount was then reduced to keep the stability limit under control. Thus, a closed-loop control for the ignition timing was achieved by monitoring the wall temperature (heat transfer rate) and the rate of hydrogen addition, in addition to the inlet temperature and fuel composition.

5.6. Heat transfer model

The heat transfer model plays an important role in combustion: it affects ignition timing; combustion duration; formation of CO, UHC and NO_x; and the rate of in-cylinder pressure and temperature rise, which is correlated to knock [174,175]. The influence of the heat loss through the combustion walls could be added in any of the numerical models discussed earlier. Some of the most commonly used heat transfer models are those devised by Anand, Woschni, Prandtl, Assanis and Hohenberg as in [176–178] and readers are advised to look at the work by Soyhan et al. [178], which explains the heat transfer equations by Assanis, Woschni and Hohenberg. From the study by Soyhan et al. [178], the Hohenberg model performs best in comparison with the Woschni and Assanis models: it predicted the in-cylinder pressure closest to the experiment, as shown in Fig. 19.

5.7. Turbulence models: RANS vs. LES

Turbulent flow occurs at high Reynolds numbers and, according to Tennekes and Lumley [179], the nature of the turbulence can be characterized as “irregularity, diffusivity, three-dimensional vorticity

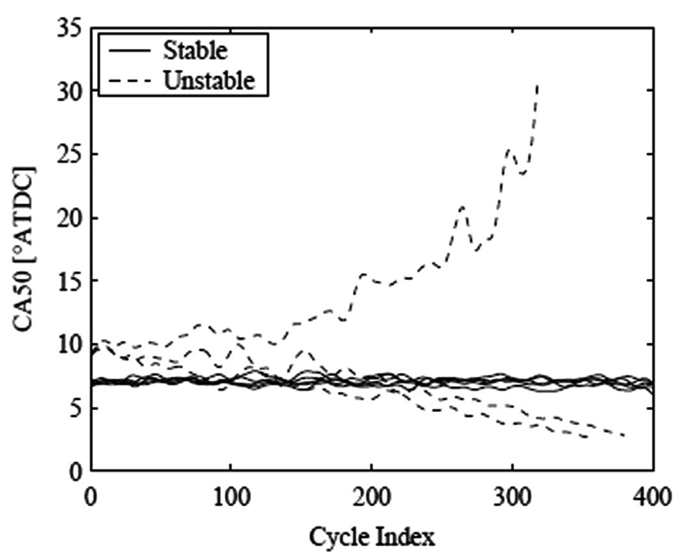


Fig. 18. Ignition timing stability captured over time-lapse [36].

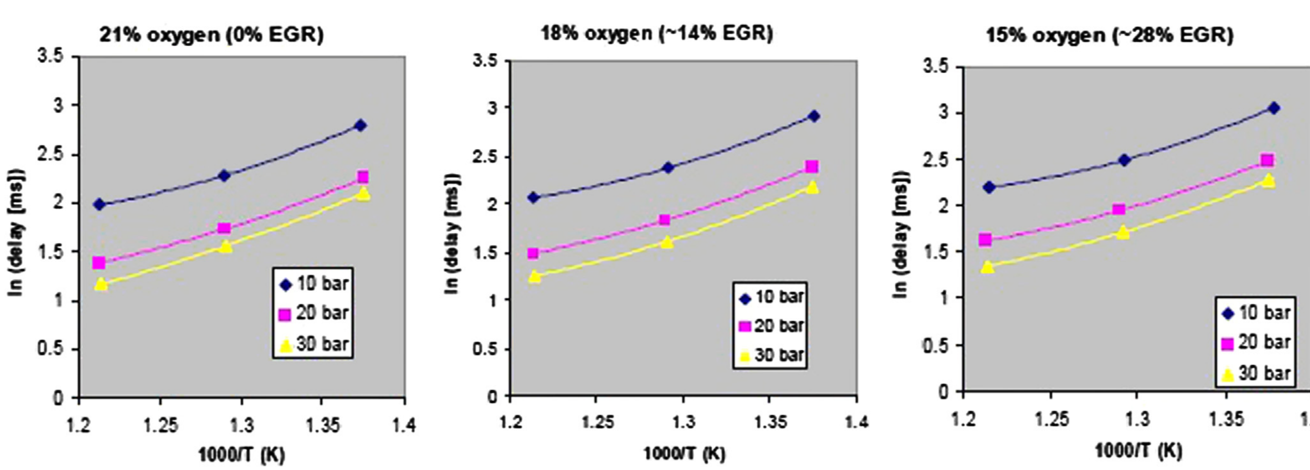


Fig. 17. Effect of EGR on ignition delay for *n*-heptane fuel [130].

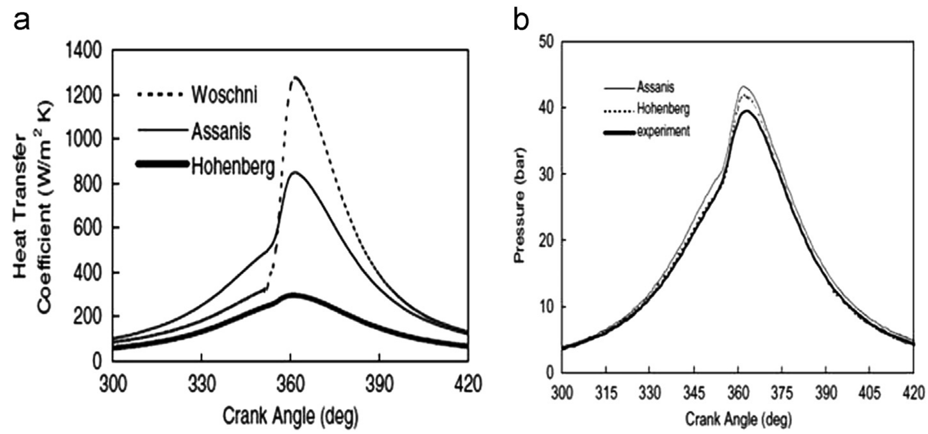


Fig. 19. Heat transfer model comparison with experiment: (a) heat transfer coefficient and (b) in-cylinder temperature difference, reproduced from [178].

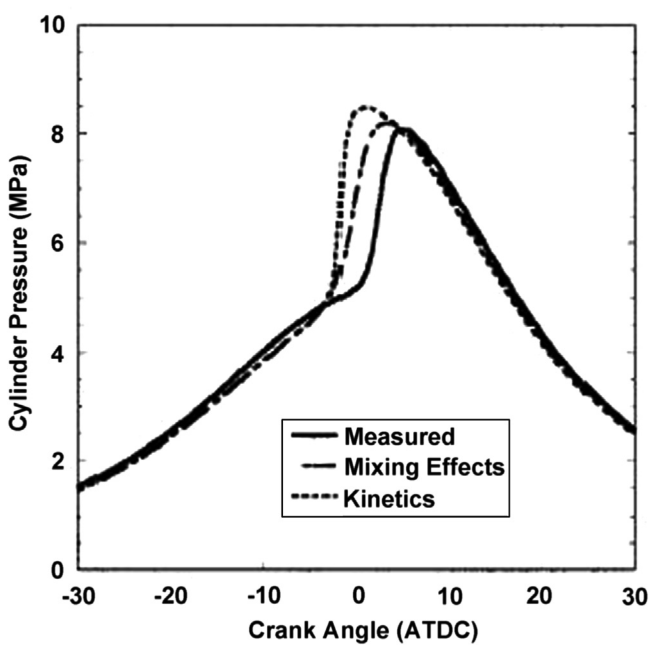


Fig. 20. The in-cylinder pressure comparison for experiment, modeling with chemical kinetics only and modeling with both chemical kinetics and turbulent mixing, reproduced from [4].

fluctuations, large Reynolds number and continuum phenomenon (continuous in space and time)". Currently there is no exact solution for most turbulent flows and this has led to the creation of turbulence models, where the useful methods to analyze the equation of motion is using statistical techniques [180,181]. The simplest statistical technique is to consider the average of flow variables over time. In HCCI engines, a piston-crown design is important to create turbulent behavior inside the combustion chamber. A study by Kong et al. [64] found that the square-bowl piston generates higher turbulence levels and results in a longer combustion duration, where the turbulence affects the combustion through its influence on the wall heat transfer and property transport. This is supported by Aceves et al. [182] with their experimental data, where the square-bowl piston resulted in a longer combustion duration but with higher UHC and CO emissions and lower combustion efficiency as a result of the thicker boundary layer. Therefore, one has to pay particular attention when designing the piston crown to achieve the desired combustion behavior. Another study by Kong and Reitz [4] revealed that including the turbulent mixing effects gave better predictions for in-cylinder pressure compared to the chemistry alone, as shown in Fig. 20. The link between chemistry and mixing effects with turbulence models is illustrated in Fig. 21.

Reynolds-Averaged Navier-Stokes (RANS) turbulence models are used in transient fluid flows, whereby the flow variables are decomposed into average and fluctuating quantities over regions in physical space that are of the order of the integral length scale [180]. Different classes of RANS models exist: zero-equation models, one-equation models, two-equation models and stress-equation models [185]. RANS models have their disadvantages, whereby: (1) they are not able to properly predict simple free-shear layers and are known to be inadequate in complex flows [185,186]; (2) they are unable to capture dynamically evolving fine-scale vortical and scalar structures due to turbulence model induced dissipation on the in-cylinder unsteady mixing process [187]; (3) the k-ε model has poor performance when used in unsteady flows, where the model over-predicts the turbulent length scales resulting in a high wall shear stress [188,189]. This is supported by Celik et al. [190], where it performs poorly when applied to IC engines with the predictions being less accurate than desired.

Large Eddy Simulation (LES), on the other hand, is a turbulence model that computes more turbulent length scales than RANS, with the turbulent energy within the inertial sub-range separated into resolved large-scale eddies and unresolved small-scale eddies. Resolved large-scale eddies are computed directly by the discretized equations, while small-scale unresolved eddies, which contain only a small fraction of the turbulent kinetic energy, are modeled through subgrid scale models. LES equations are obtained by appropriate filtering of the Navier-Stokes equations and the energy equations over a three-dimensional space [190]. In complex flows for nonreactive and reactive system studies, LES predicts the scalar mixing process and dissipation rates with considerably improved accuracy compared to RANS [191]. It offers a more realistic representation of the in-cylinder turbulent flow and delivers accurate predictions for non-premixed combustion [184,192].

However, LES has difficulties in the near-wall region, where the mesh should be fine enough to compute a correct shear stress [184,193]. Furthermore, results from LES may introduce serious errors into simulations due to both aliasing and truncation errors of low-order schemes, which can degrade LES computations [180]. Therefore, LES requires greater mesh refinement compared to RANS, which increases the computational cost. However, mesh or time-step refinement in RANS improves the numerical accuracy, but does not improve the scales that are resolved. Instead, it converges to an exact solution of the filtered Navier-Stokes equations, while LES converges towards the unfiltered Navier-Stokes equations [192].

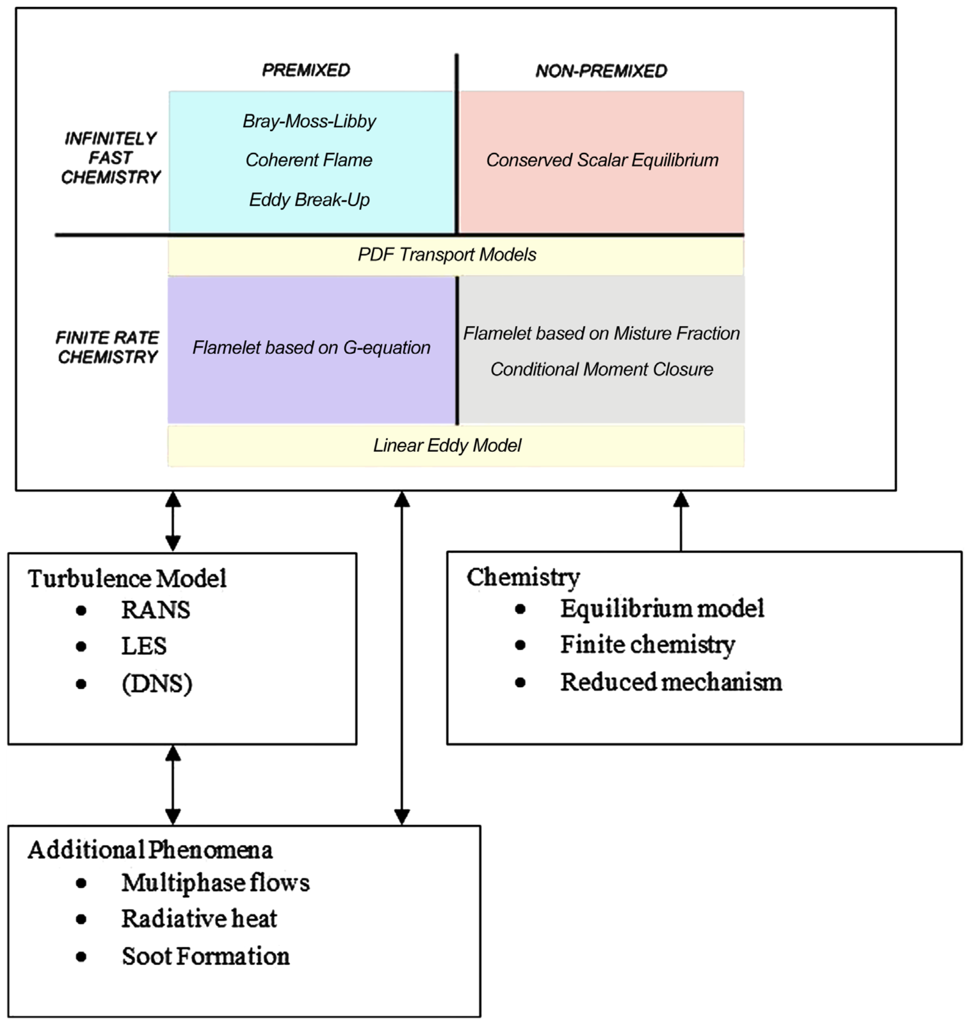


Fig. 21. Illustration of an overall model for transient simulations [180,183,184].

A hybrid approach between RANS and LES has been created in order to resolve the disadvantages of these two models. Alfonsi [185] has categorized this approach into zonal decomposition, nonlinear disturbance equations and universal modeling. Benarafa et al. [193] in their study on the hybrid approach, which they called RANS/LES coupling, shows that this approach seems to correctly force the averaged LES velocity to reach the correct steady RANS velocity field even at high Reynolds numbers. The fluctuations are globally improved despite the use of very coarse meshes.

Another approach which is similar to the hybrid RANS–LES model is called Detached Eddy Simulation (DES). DES, which is already included in commercial CFD packages, implements the RANS approach near the wall region, while using the LES technique in the outer detached eddies. The main objective of using this technique is to avoid using high resolution in the near-wall region, and therefore, reduce computational cost. Instead, algebraic boundary-layer models (which have proven to be very successful in the RANS context) are implemented.

5.8. Mixing models for non-premixed combustion

Turbulent mixing will take place when there is inhomogeneity in the mixture and depends on the geometry of the piston crown. Fuels and oxidizers are required to be mixed at molecular levels to initiate combustion, while the molecular mixing will take place at the interface between small eddies [180,191]. This process will heavily involve the chemical reactions, which leads to the diffusion process.

The Euclidean Minimum Spanning Tree (EMST) [194] mixing model is designed to overcome shortcomings of simpler turbulent mixing models, and was successful in diffusion flame tests [194,195]. The problem with simpler models is that the mixing occurs between particles across the reaction zone, which is not local. The EMST model only allows the particles to mix between their immediate neighbors in composition space. The model was constructed by connecting particles to form branches of trees over the timestep. The particles enter or leave the cell according to their velocity. Each of the particles has its own age property and this determines whether the particle belongs to the mixing or non-mixing state. If the particle age property is positive, it belongs to the mixing state, while it is not if the age property is zero or negative. The EMST is formed on the mixing state and changes discontinuously in time due to the particles entering or leaving the mixing state.

Mitarai et al. [195] conducted a performance comparison between EMST, Interaction by Exchange with the Mean (IEM) [196] and the Modified Curl's (MC) [197] mixing models in RANS and LES environments and found the EMST mixing model yielded significantly better results than the IEM and MC mixing models.

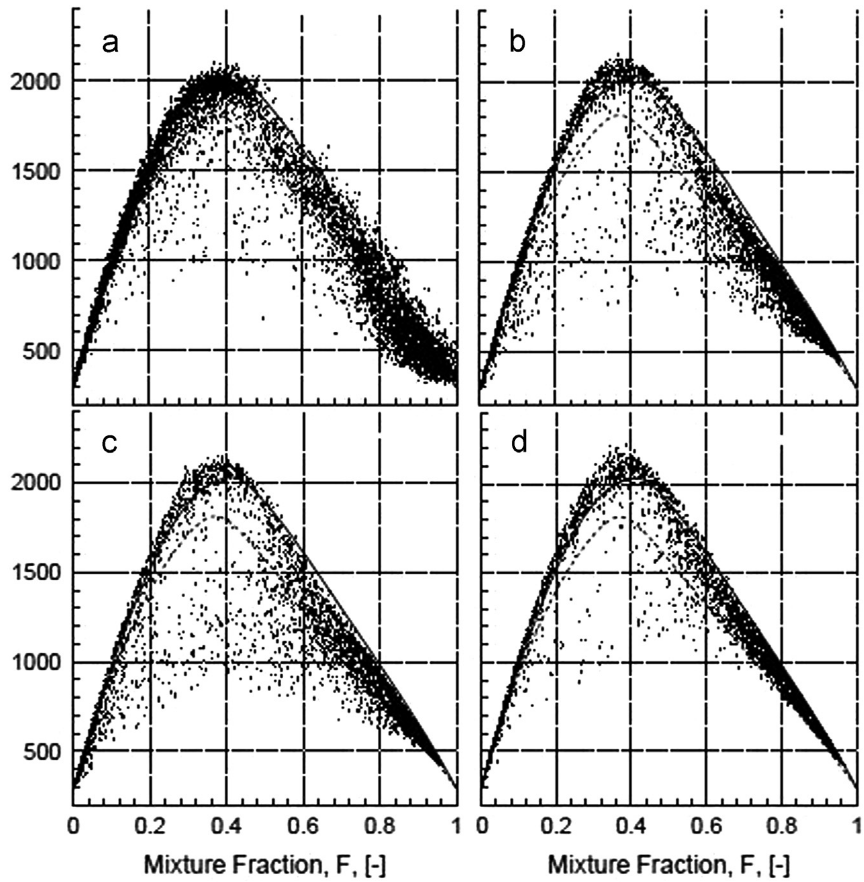


Fig. 22. Scatter plots of temperature vs. mixture fraction from experiment and simulations using LES: (a) experimental data, (b) IEM, (c) MC and (d) EMST. All figures reproduced from [198].

It was found that the EMST mixing model performs better in an LES environment than in a RANS environment. This is because of the ability of LES to resolve finer scales compared to RANS and therefore particle interactions are over finer scales [198]. The EMST mixing model has also successfully predicted the appearance and disappearance of cold particles in LES, where it has failed in RANS. A study of turbulence and chemistry interaction performed by Bisetti and Chen [198] showed that the EMST in the LES environment performed better than the IEM and MC in predicting the temperature conditioned on the mixture fraction, as shown in Fig. 22.

Bisetti et al. [199] studied turbulence and chemistry interactions in HCCI engines using the same models as Mitarai et al. [195]. They found that the EMST mixing model performed better than the other mixing models. They noted that the LES simulation gives a promising step in HCCI engine modeling under high levels of stratification.

The Probability Density Function (PDF) [200] method offers a good advantage in modeling turbulent reactive flows, where it has the ability to capture strong turbulence-chemistry interactions in the mixing models, such as IEM, MC or EMST [201]. But, this model is hard to solve because it has many dimensions: one for each chemical species in a particular set of chemical reactions. Therefore, it will end up with n dimensions for n chemical species and if there are m nodes per dimension, the total number of nodes will be m^n, resulting in an enormous computational cost, which is why it is always solved stochastically. The Conditional Moment Closure (CMC) [202] model on the other hand, was designed to handle turbulence chemistry interactions, where large chemical mechanisms can be used at modest computational cost. The conditional fluctuations of the reactive components are to be neglected when calculating the chemical source term for first-order CMC: the value is significantly smaller than the unconditional fluctuations [203]. Bushe and Steiner [204] implemented the CMC model in the LES environment for non-premixed turbulent reacting flows. They noted that the resolution constraints were reduced because the chemical reactions are resolved in the mixing space. However, the CMC model has a disadvantage in modeling the properties′ fluctuations since it has only one conditioning variable [205].

The MMC model [205] was designed to solve the difficulties faced by the PDF method and the CMC model. It combines the precepts of PDF modeling (in modeling the major species) and CMC (for the minor species) while treating the complete set of dependent variables equally [205]. The major species are solved by mapping them to a set of prescribed reference variables (often standard Gaussian in the conventional description), while fluctuations of minor species are either ignored (conditional MMC) or treated with conventional mixing models (probabilistic MMC) [206].

An investigation of MMC, studying the same case as Mitarai et al. [195], reported that the model is capable of predicting the mean temperature rise with reasonable fidelity and follows the temperature history at stoichiometric mixture fraction better than the other models [207], as shown in Fig. 23. A study by Cleary and Kronenburg [206] for the MMC model in turbulent diffusion flames shows an improved accuracy in local extinction of chemical time scales compared to the CMC model. Vogiatzaki et al. [208] tested the MMC model for inhomogeneous reactive flows in turbulent jet diffusion flames. The model was constructed using a one-dimensional reference space with mixture fraction used as a basis for the reference variable. They found that the temperature

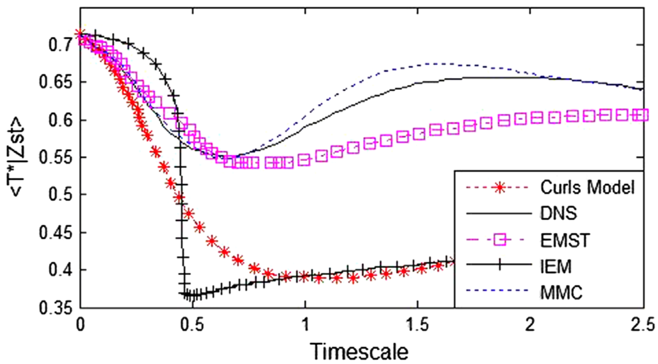


Fig. 23. Temperature at stoichiometric mixture fraction for various mixing models [195,207].

was predicted well compared to the experiment at all locations. In addition, Vogiatzaki et al. [209] mentioned that the MMC model could be easily included in an LES turbulent model. This was done by Cleary et al. [210] where they used the MMC model with an LES scheme for turbulent diffusion flames. The LES model was used to solve for the turbulent velocity field and the reference mixture fraction, while the stochastic MMC model solved the reactive scalars. They concluded that the conditional averages of temperature and species were in good agreement with the experiment.

The advantages of using the MMC model [209,211] are: (1) the simplicity of modeling the MMC diffusion coefficients against other models, (2) conditional scalar dissipation rates appears in closed form and (3) no need to presume the mixture fraction PDF because it is computed from the modeling of the relationship between mixture fraction and reference variable. However, there is difficulty in modeling the MMC, where the model cannot generate fluctuations around the conditional mean for the joint PDF, and an additional transport equation is necessary to impose the conditional fluctuations [212]. In other words, the MMC method looks to be a promising step in developing a mixing model for HCCI engines.

6. Conclusion

It can be clearly seen that the hydrogen-diesel combination in HCCI engines shows better results for most major quantities, while producing a higher efficiency compared to the single diesel mode and the natural gas–diesel mode. A higher BTE will help reduce the fuel consumption of the engine and it might be able to match the fuel consumption of a hybrid engine. If the HCCI engine is used in a hybrid configuration, it might help reduce the fuel consumption even further. It looks like a promising choice of engines in the near future.

The HCCI engine has low emissions levels of NO_x, soot and particulates. However, HCCI engines still have unresolved issues, which are knocking and high levels of unburned HC and CO emissions. If hydrogen is added to diesel-air mixture, knocking will take place once the energy ratio is more than 16%. It is expected that the knocking in HCCI engines is influenced by chemical kinetics, where the combustion is no longer controlled by the injection or the spark timing. Therefore, it is hypothesized that the knocking in HCCI engines could be due to the region with the highest OH concentrations in the high temperature zone, where the highest temperature region will initiate instantaneous local combustion resulting in a local high heat release rate. Further studies have to be performed in order to solve these remaining issues. To achieve this, the numerical method shows a great advantage over experiments to simulate the combustion behavior in terms of cost and time. To this end, a simulation model has to be developed to investigate the behavior and, once complete, it has to be validated against experiments.

The multi-zone numerical method combined with advanced turbulent mixing models shows promising results, compared with the single-zone model. CFD offers greater accuracy than the multi-zone model at the expense of computational cost. But, one could easily implement the LES or DES model with CFD. The DES model will be useful in the near future, where it combines the LES and RANS models together with improved accuracy using the former where needed and improved computational efforts using the latter where possible. A mixing model has been developed to study the mixing behavior at molecular levels. The performance of EMST, MC and IEM models were compared and it showed that the EMST model performed best. A study of the CMC model showed that it has the ability to capture all phases of combustion, i.e. ignition, flame propagation and a diffusion flame [213]. A CMC model in an LES environment has been investigated, and it shows that the model has the capability to predict extinction and ignition phenomena [204]. The MMC model is created by combining the advantages of the CMC and PDF models. Therefore, the MMC model is expected to deliver a better result if it is implemented in a DES environment, as both models exist to use the advantage of other models.

There are several methods to achieve HCCI configurations through experiments. Using a direct injection system seems to require few modifications, but care is required with the associated disadvantages. If port injection is to be used, one might have to install the atomizer and heater in the inlet port, which leads to additional costs. The main objective of the HCCI engine is to achieve a high compression ratio, which provides similar efficiency to the CI engine or better, with emissions levels at least as good as SI engines. Therefore, an optimized experimental method would be able to solve the HCCI engine problems, with the help of simulations. The major problem yet to be solved is knocking, thus it is imperative to develop a model so that HCCI engines can be used in the near future.

References

[1] Rattanapaibule K, Aung K. Performance predictions of a hydrogen-enhanced natural gas HCCI engine. In: Proceedings of the international mechanical engineering congress and exposition (IMECE2005). Energy Conversion and Resources. Florida; 2005. p. 89–294.

[2] Epping K, Aceves S, Bechtold R, Dec J. The potential of HCCI combustion for high efficiency and low emissions. SAE Paper 2002-01-1923; 2002.

[3] Christensen M, Johansson B. Influence of mixture quality on homogeneous charge compression ignition. SAE paper 982454; 1998.

[4] Kong SC, Reitz RD. Use of detailed chemical kinetics to study HCCI engine combustion with consideration of turbulent mixing effects. J Eng Gas Turbines Power 2002;124:702–7.

[5] Najt PE, Foster DE. Compression ignited homogeneous charge combustion. SAE Paper 830264; 1983.

[6] Kong SC, Reitz RD. Numerical study of premixed HCCI engine combustion and its sensitivity to computational mesh and model uncertainties. Combust Theor Model 2003;7:417–33.

[7] Soylu S. Examination of combustion characteristics and phasing strategies of a natural gas HCCI engine. Energy Convers Manag 2005;46:101–19.

[8] Killingsworth NJ, Aceves SM, Flowers DL, Krstic M. A simple HCCI engine model for control. IEEE Int Conf Control 2006:1479–84.

[9] Mack JH, Aceves SM, Dibble RW. Demonstrating direct use of wet ethanol in a homogeneous charge compression ignition (HCCI) engine. Energy 2009;34:782–7.

[10] Aceves S, Flowers D. Engine shows diesel efficiency without the emissions. Sci Technol Rev 2004:17–9.

[11] Christensen M, Johansson B, Einewall P. Homogeneous charge compression ignition (HCCI) using iso-octane, ethanol and natural gas – a comparison with spark ignition operation. SAE Paper 971676; 1997.

[12] Hiltner J, Fiveland SB, Agama R, Willi M. System efficiency issues for natural gas fueled HCCI engines in heavy-duty stationary applications. SAE Paper 2002-01-0417; 2002.

[13] Kawano D, Suzuki H, Ishii H, Goto Y, Odaka M, Murata Y, et al. Ignition and combustion control of diesel HCCI. SAE Paper 2005-01-2132; 2005.

[14] Nathan SS, Mallikarjuna JM, Ramesh A. An experimental study of the biogas-diesel HCCI mode of engine operation. Energy Convers Manag 2010;51:1347–53.
[15] Yap D, Peucheret SM, Megaritis A, Wyszynski ML, Xu H. Natural gas HCCI engine operation with exhaust gas fuel reforming. Int J Hydrogen Energy 2006;31:587–95.
[16] Jun D, Ishii K, Iida N. Autoignition and combustion of natural gas in a 4 stroke HCCI engine. JSME Int J B-Fluid Therm Eng 2003;46:60–7.
[17] Volkswagen. Volkswagen Aktiengesellschaft – Annual Report. Wolfsburg; 2009.
[18] Audi. 2012. URL: 〈http://www.audi.com/com/brand/en/tools/advice/glossary/fsi.browser.html〉 [accessed 19.04.12].
[19] Barber EM, Reynolds B, Tierney WT. Elimination of combustion knock-Texaco combustion process, SAE paper 510173; 1951.
[20] Takagi Y. A new era in spark-ignition engines featuring high-pressure direct injection. In: Proceeding of the twenty-seventh international symposium on combustion. The Combustion Institute; 1998. p. 2055–68.
[21] Yao MF, Zheng ZL, Liu HF. Progress and recent trends in homogeneous charge compression ignition (HCCI) engines. Prog Energy Combust Sci 2009;35:398–437.
[22] Premier. HCCI could cut fuel consumption by 15%, Adv Mater Process. 2004; 165, (11), 27.
[23] Papagiannakis RG, Hountalas DT. Combustion and exhaust emission characteristics of a dual fuel compression ignition engine operated with pilot diesel fuel and natural gas. Energy Convers Manag 2004;45:2971–87.
[24] Tobin J, Carlson ME, Elias MJ, Keene WR, O'Sullivan JP, Tita MJ, et al. Natural gas 1998. Issues and trends. Washington: Energy Information Administration (EIA); 1999.
[25] Cho HM, He BQ. Spark ignition natural gas engines – a review. Energy Convers Manag 2007;48:608–18.
[26] Flowers D, Aceves S, Westbrook CK, Smith JR, Dibble R. Detailed chemical kinetic simulation of natural gas HCCI combustion: gas composition effects and investigation of control strategies. J Eng Gas Turb Power 2001;123:433–9.
[27] Rousseau S, Lemoult B, Tazerout M. Combustion characterization of natural gas in a lean burn spark-ignition engine. Proc Inst Mech Eng D—J Automob Eng 1999;213:481–9.
[28] Zeng K, Huang ZH, Liu B, Liu LX, Jiang DM, Ren Y, et al. Combustion characteristics of a direct-injection natural gas engine under various fuel injection timings. Appl Therm Eng 2006;26:806–13.
[29] Duc PM, Wattanavichien K. Study on biogas premixed charge diesel dual fuelled engine. Energy Convers Manag 2007;48:2286–308.
[30] Saravanan N, Nagarajan G. An experimental investigation on hydrogen fuel injection in intake port and manifold with different EGR rates. Energy Environ 2010;1:221–48.
[31] Fiveland SB, Assanis DN. A four-stroke homogeneous charge compression ignition engine for combustion and performance studies. SAE Paper 2000-01-0332; 2000.
[32] Jahirul MI, Masjuki HH, Saidur R, Kalam MA, Jayed MH, Wazed MA. Comparative engine performance and emission analysis of CNG and gasoline in a retrofitted car engine. Appl Therm Eng 2010;30:2219–26.
[33] Mercuri R, Bauen A, Hart D. Options for refuelling hydrogen fuel cell vehicles in Italy. J Power Sour 2002;106:353–63.
[34] Johannes VE, Tom P, Nicholas H, Giorgio S, Giancarlo T. Liquid petroleum gas and natural gas combustion engines. In: OECD I, editor. Technology brief T03: energy technology system analysis program; June 2009.
[35] Jonathan P. Responses to questions on the design elements of a mandatory market-based greenhouse gas regulatory system. U.S Senate Committee on Energy and Natural Resources, Washington; 2006.
[36] Olsson J-O, Tunesta P, Johansson B, Fiveland SB, Agama R, Willi M, et al. Compression ratio influence on maximum load of a natural gas fueled HCCI engine. SAE Paper 02P-147; 2002.
[37] Ramli MZ. Adsoprtion of natural gas and hydrogen on Cu3. Malaysia: University Malaysia Pahang; 2009.
[38] Chemical Safety Data Sheet. Malaysia: Gas Malaysia; 2011.
[39] Antunes JMG, Mikalsen R, Roskilly AP. An investigation of hydrogen-fuelled HCCI engine performance and operation. Int J Hydrogen Energy 2008;33:5823–8.
[40] Szwaja S, Grab-Rogalinski K. Hydrogen combustion in a compression ignition diesel engine. Int J Hydrogen Energy 2009;34:4413–21.
[41] Saravanan N, Nagarajan G, Sanjay G, Dhanasekaran C, Kalaiselvan KM. Combustion analysis on a DI diesel engine with hydrogen in dual fuel mode. Fuel 2008;87:3591–9.
[42] Park C, Kim C, Kim K, Lee D, Song Y, Moriyoshi Y. The influence of hydrogen-enriched gas on the performance of lean NO(x) trap catalyst for a light-duty diesel engine. Int J Hydrogen Energy 2010;35:1789–96.
[43] Peucheret S, Wyszynski ML, Lehrle RS, Golunski S, Xu H. Use of catalytic reforming to aid natural gas HCCI combustion in engines: experimental and modelling results of open-loop fuel reforming. Int J Hydrogen Energy 2005;30:1583–94.
[44] Komninos NP, Hountalas DT, Kouremenos DA. Development of a new multi-zone model for the description of physical processes in HCCI engines. SAE Paper 2004-01-0562; 2004.
[45] Pitz WJ, Cernansky NP, Dryer FL, Egolfopoulos FN, Farrell JT, Friend DG, et al. Development of an experimental database and chemical kinetic models for surrogate gasoline fuels. SAE Paper 2007-01-0175; 2007.
[46] Naik CV, Pitz WJ, Sjoberg M, Dec JE, Orme J, Curran HJ, et al. Detailed chemical kinetic modeling of surrogate fuels for gasoline and application to an HCCI engine. Joint meeting of the US Sections of the Combustion Institute. Philadelphia, United States: Lawrence Livermore National Laboratory; 2005.
[47] Komninos NP, Rakopoulos CD. Modeling HCCI combustion of biofuels: a review. Renew Sust Energy Rev 2012;16:1588–610.
[48] (de) Risi A, Carlucci AP, Laforgia D, Naccarato F. Experimental investigation and combustion analysis of a direct injection dual-fuel diesel-natural gas engine. Energy 2008;33:256–63.
[49] Saravanan N, Nagarajan G, Narayanasamy S. An experimental investigation on DI diesel engine with hydrogen fuel. Renew Energy 2008;33:415–21.
[50] Verhelst S, Wallner T. Hydrogen-fueled internal combustion engines. Prog Energy Combust Sci 2009;35:490–527.
[51] Kong SC. A study of natural gas/DME combustion in HCCI engines using CFD with detailed chemical kinetics. Fuel 2007;86:1483–9.
[52] Tomita E. Dual fuel HCCI combustion – high octane and high cetane number fuels. In: Proceedinhs of the HCCI symposium. Berkeley: Okayama University; 2004.
[53] Tomita E, Kawahara N, Piao Z, Fujita S, Hamamoto Y. Hydrogen combustion and exhaust emissions ignited with diesel oil in a dual fuel engine. SAE paper 2001-01-3503; 2001.
[54] Tomita E, Kawahara N, Piao Z, Yamaguchi R. Effects of EGR and early injection of diesel fuel on combustion characteristics and exhaust emissions in a methane duel fuel engine. SAE Paper 2002-01-2723; 2002.
[55] Liu C, Karim GA. A simulation of the combustion of hydrogen in HCCI engines using a 3D model with detailed chemical kinetics. Int J Hydrogen Energy 2008;33:3863–75.
[56] Amneus P, Nilsson D, Mauss F, Christensen M, Johansson B. Homogeneous charge compression ignition engine: experiments and detailed kinetic calculations. In: Proceedings of the fourth international symposium. COMODIA; 1998. p. 567–72.
[57] Antunes JMG, Mikalsen R, Roskilly AP. An experimental study of a direct injection compression ignition hydrogen engine. Int J Hydrogen Energy 2009;34:6516–22.
[58] Garcia MT, F.J.J.E. Aguilar, Lencero TS. Experimental study of the performances of a modified diesel engine operating in homogeneous charge compression ignition (HCCI) combustion mode versus the original diesel combustion mode. Energy 2009;34:159–71.
[59] Zheng QP, Zhang HM, Zhang DF. A computational study of combustion in compression ignition natural gas engine with separated chamber. Fuel 2005;84:1515–23.
[60] Tsolakis A, Megaritis A. Partially premixed charge compression ignition engine with on-board H-2 production by exhaust gas fuel reforming of diesel and biodiesel. Int J Hydrogen Energy 2005;30:731–45.
[61] EPA. Control of air pollution from new motor vehicles: tier 2 motor vehicle emissions standards and gasoline sulfur control requirements. United States: U.S. Environmental Protection Agency; 2000.
[62] Popp D. International innovation and diffusion of air pollution control technologies: The effects of NO_x and SO_2 regulation in the U.S., Japan, and Germany. Cambridge: National Bureau of Economic Research; 2004.
[63] Wesselink LG, Buijsman E, Annema JA. The impact of Euro 5: facts and figures. The Netherlands; 2006.
[64] Kong SC, Reitz RD, Christensen M, Johansson B. Modeling the effects of geometry generated turbulence on HCCI engine combustion. SAE Paper 2003-01-1088; 2003.
[65] Meca. Emission control technology for stationary internal combustion engines. Washington: Manufacturers of Emissions Controls Association (MECA); 1997.
[66] Rizvi SQA. A comprehensive review of lubricant chemistry, technology, selection and design. U.S.A.: ASTM International; 2009.
[67] Ganesh D, Nagarajan G. Homogeneous charge compression ignition (HCCI) combustion of diesel fuel with external mixture formation. Energy 2010;35:148–57.
[68] Park SW, Reitz RD. Numerical study on the low emission window of homogeneous charge compression ignition diesel combustion. Combust Sci Technol 2007;179:2279–307.
[69] Ganesh D, Nagarajan G, Ibrahim MM. Study of performance, combustion and emission characteristics of diesel homogeneous charge compression ignition (HCCI) combustion with external mixture formation. Fuel 2008;87:3497–503.
[70] Bression G, Soleri D, Savy S, Dehoux S, Azoulay D, Hamouda HB, et al. A study of methods to lower HC and CO emissions in diesel HCCI. SAE Paper 2008-01-0034; 2008.
[71] Heywood JB. Internal combustion engine fundamentals. United States of America: McGraw-Hill; 1988.
[72] Komninos NP. Investigating the importance of mass transfer on the formation of HCCI engine emissions using a multi-zone model. Appl Energy 2009;86:1335–43.
[73] He BQ, Cho HM. Spark ignition natural gas engines – a review. Energy Convers Manag 2007;48:608–18.
[74] Li H, Neill WS, Chippior W, Graham L, Connolly T, Taylor JD. An experimental investigation on the emission characteristics of HCCI engine operation using *n*-heptane. SAE Paper 2007-01-1854; 2007.
[75] Stone R. Introduction to internal combustion engines. 3rd ed.. Warrendale: Society of Automotive Engineers Inc; 1999.
[76] Kuo KK. Principles of combustion. New Jersey: John Wiley and Sons; 2005.
[77] Sjoberg M, Dec JE. An investigation into lowest acceptable combustion temperatures for hydrocarbon fuels in HCCI engines. Proc Combust Inst 2005;30:2719–26.

[78] Alkidas AC. Combustion advancements in gasoline engines. Energy Convers Manag 2007;48:2751–61.
[79] Aceves SM, Flowers DL, Martinez-Frias J, Smith JR, Dibble R, Au M, et al. HCCI combustion: analysis and experiments. SAE Paper 2001-01-2077; 2001.
[80] Miller JA, Bowman CT. Mechanism and modeling of nitrogen chemistry in combustion. Prog Energy Combust Sci 1989;15:287–338.
[81] Tanaka S, Ayala F, Keck JC. A reduced chemical kinetic model for HCCI combustion of primary reference fuels in a rapid compression machine. Combust Flame 2003;133:467–81.
[82] Ma JJ, Lu XC, Ji LB, Huang Z. An experimental study of HCCI-DI combustion and emissions in a diesel engine with dual fuel. Int J Therm Sci 2008;47:1235–42.
[83] Soberanis MAE, Fernandez AM. A review on the technical adaptations for internal combustion engines to operate with gas/hydrogen mixtures. Int J Hydrogen Energy 2010;35:12134–40.
[84] Akansu SO, Dulger Z, Kahraman N, Veziroglu TN. Internal combustion engines fueled by natural gas - hydrogen mixtures. Int J Hydrogen Energy 2004;29:1527–39.
[85] Van Blarigan P. Advanced internal combustion electrical generator. DOE hydrogen program review NREL/CP-610-32405. United States; 2002.
[86] Yusaf TF, Buttsworth DR, Saleh KH, Yousif BF. CNG-diesel engine performance and exhaust emission analysis with the aid of artificial neural network. Appl Energy 2010;87:1661–9.
[87] Tsolakis A, Megaritis A, Yap D. Application of exhaust gas fuel reforming in diesel and homogeneous charge compression ignition (HCCI) engines fuelled with biofuels. Energy 2008;33:462–70.
[88] Kayes D, Hochgreb S. Mechanism of particulate matter formation in spark-ignition engines. 3. Model of PM formation. Environ Sci Technol 1999;33:3978–92.
[89] Kayes D, Hochgreb S. Mechanisms of particulate matter formation in spark-ignition engines. 1. Effect of engine operating conditions. Environ Sci Technol 1999;33:3957–67.
[90] Carlucci AP, de Risi A, Laforgia D, Naccarato F. Experimental investigation and combustion analysis of a direct injection dual-fuel diesel-natural gas engine. Energy 2008;33:256–63.
[91] Hyvonen J, Haraldsson G, Johansson B. Operating range in a multi cylinder HCCI engine using variable compression ratio. SAE Paper 2003-01-1829; 2003.
[92] Roy MM, Tomita E, Kawahara N, Harada Y, Sakane A. An experimental investigation on engine performance and emissions of a supercharged H-2-diesel dual-fuel engine. Int J Hydrogen Energy 2010;35:844–53.
[93] Stiesch G. Modeling engine spray and combustion processes. Berlin: Springer; 2003.
[94] Guo HS, Hosseini V, Neill WS, Chippior WL, Dumitrescu CE. An experimental study on the effect of hydrogen enrichment on diesel fueled HCCI combustion. Int J Hydrogen Energy 2011;36:13820–30.
[95] Shudo T, Yamada H. Hydrogen as an ignition-controlling agent for HCCI combustion engine by suppressing the low-temperature oxidation. Int J Hydrogen Energy 2007;32:3066–72.
[96] Ryu J, Kim H, Lee K. A study on the spray structure and evaporation characteristic of common rail type high pressure injector in homogeneous charge compression ignition engine. Fuel 2005;84:2341–50.
[97] Kim MY, Lee CS. Effect of a narrow fuel spray angle and a dual injection configuration on the improvement of exhaust emissions in a HCCI diesel engine. Fuel 2007;86:2871–80.
[98] Roy MM, Tomita E, Kawahara N, Harada Y, Sakane A. Performance and emission comparison of a supercharged dual-fuel engine fueled by producer gases with varying hydrogen content. Int J Hydrogen Energy 2009;34:7811–22.
[99] Liu Z. Diesel combustion chamber. In: Company IEIP, editor. United States Patent. United States; 2006.
[100] Morsy MH. Ignition control of methane fueled homogeneous charge compression ignition engines using additives. Fuel 2007;86:533–40.
[101] Fiveland SB, Assanis DN. Development and validation of a quasi-dimensional model for hcci engine performance and emissions studies under turbocharged conditions. SAE Paper 2002-01-1757; 2002.
[102] Reitz RD. CFD combustion models for IC engines. Madison: The University of Wisconsin; 2007.
[103] Tanaka S, Ayala F, Keck JC, Heywood JB. Two-stage ignition in HCCI combustion and HCCI control by fuels and additives. Combust Flame 2003;132:219–39.
[104] Agarwal A, Assanis DN. Multi-dimensional modeling of natural gas ignition under compression ignition conditions using detailed chemistry. In: Proceedings of the international congress and exposition. Michigan: SAE Paper 980136; 1998.
[105] Liu HG, Yao MF, Zhang B, Zheng ZQ. Influence of fuel and operating conditions on combustion characteristics of a homogeneous charge compression ignition engine. Energy Fuel 2009;23:1422–30.
[106] Najjar YSH. Hydrogen safety: the road toward green technology. Int J Hydrogen Energy 2013;38:10716–28.
[107] Sun ZY, Liu FS, Liu XH, Sun BG, Sun DW. Research and development of hydrogen fuelled engines in China. Int J Hydrogen Energy 2012;37:664–81.
[108] Saravanan N, Nagarajan G. An experimental investigation of hydrogen-enriched air induction in a diesel engine system. Int J Hydrogen Energy 2008;33:1769–75.
[109] de Morais AM, Mendes Justino MA, Valente OS, SdM Hanriot, Sodré JR. Hydrogen impacts on performance and CO_2 emissions from a diesel power generator. Int J Hydrogen Energy 2013;38:6857–64.
[110] Fayaz H, Saidur R, Razali N, Anuar FS, Saleman AR, Islam MR. An overview of hydrogen as a vehicle fuel. Renew Sust Energy Rev 2012;16:5511–28.
[111] Christodoulou F, Megaritis A. Experimental investigation of the effects of separate hydrogen and nitrogen addition on the emissions and combustion of a diesel engine. Int J Hydrogen Energy 2013;38:10126–40.
[112] Bromberg L, Cohn DR, Rabinovich A, Heywood J. Emissions reductions using hydrogen from plasmatron fuel converters. Int J Hydrogen Energy 2001;26:1115–21.
[113] Bari S, Esmaeil MM. Effect of H_2/O_2 addition in increasing the thermal efficiency of a diesel engine. Fuel 2010;89:378–83.
[114] Frolov SM, Medvedev SN, Basevich VY, Frolov FS. Self-ignition of hydrocarbon–hydrogen–air mixtures. Int J Hydrogen Energy 2013;38:4177–84.
[115] Nguyen TA, Mikami M. Effect of hydrogen addition to intake air on combustion noise from a diesel engine. Int J Hydrogen Energy 2013;38:4153–62.
[116] Miyamoto T, Hasegawa H, Mikami M, Kojima N, Kabashima H, Urata Y. Effect of hydrogen addition to intake gas on combustion and exhaust emission characteristics of a diesel engine. Int J Hydrogen Energy 2011;36:13138–49.
[117] Agarwal A, Assanis DN. Multi-dimensional modeling of ignition, combustion and nitric oxide formation in direct injection natural gas engines. International spring fuels & lubricants. Paris: SAE Paper 011839; 2000.
[118] Babajimopoulos A, Lavoie GA, Assanis DN. Modeling HCCI combustion with high levels of residual gas fraction – a comparison of two VVA strategies. SAE Paper 2003-01-3220; 2003.
[119] Chen Z, Konno M, Goto S. Study on homogeneous premixed charge CI engine fueled with LPG. JSAE Rev 2001;22:265–70 (Paper 200114339).
[120] McTaggart-Cowan GP, Wu N, Jin B, Rogak SN, Davy MH, Bushe WK. Effects of fuel composition on high-pressure non-premixed natural gas combustion. Combust Sci Technol 2009;181:397–416.
[121] Curran HJ, Gaffuri P, Pitz WJ, Westbrook CK. A comprehensive modeling study of *n*-heptane oxidation. Combust Flame 1998;114:149–77.
[122] Curran HJ, Gaffuri P, Pitz WJ, Westbrook CK. A comprehensive modeling study of iso-octane oxidation. Combust Flame 2002;129:253–80.
[123] Golovitchev V. Mechanisms (combustion chemistry). URL: 〈http://www.tfd.chalmers.se/~valeri/MECH.html〉; 2003.
[124] Lee K, Kim Y, Min K. Development of a reduced chemical kinetic mechanism for a gasoline surrogate for gasoline HCCI combustion. Combust Theor Model 2011;15:107–24.
[125] Mehl M, Pitz WJ, Westbrook CK, Curran HJ. Kinetic modeling of gasoline surrogate components and mixtures under engine conditions. Proc Combust Inst 2011;33:193–200.
[126] William JP, Charles KW. Combustion Chemistry. California, United States. Lawrence Livermore National Laboratory; 2011 ([accessed 9.04.11]).
[127] Westbrook CK, Pitz WJ, Mehl M, Curran HJ. Detailed chemical kinetic models for large *n*-alkanes and iso-alkanes found in conventional and F-T diesel fuels. US National Combustion Meeting. Ann Arbor; 2009.
[128] Farrell JT, Cernansky NP, Dryer FL, Friend DG, Hergart CA, Law CK, et al. Development of an experimental database and kinetic models for surrogate diesel fuels. SAE Paper 2007-01-0201; 2007.
[129] Mehl M, Curran HJ, Pitz WJ, Westbrook CK. Chemical kinetic modeling of component mixtures relevant to gasoline. In: Proceedings of the 4th european combustion meeting. Vienna; 2009.
[130] Taylor JD. Fuel performance technologies: milestone FY06 9.1. National Renewable Energy Laboratory; 2006.
[131] Ra Y, Reitz RD. A reduced chemical kinetic model for IC engine combustion simulations with primary reference fuels. Combust Flame 2008;155:713–38.
[132] Guo HS, Neill WS, Chippior W, Li HL, Taylor JD. An experimental and modeling study of HCCI combustion using *n*-heptane. J Eng Gas Turb Power 2010;132:1–10.
[133] Hernandez JJ, Sanz-Argent J, Benajes J, Molina S. Selection of a diesel fuel surrogate for the prediction of auto-ignition under HCCI engine conditions. Fuel 2008;87:655–65.
[134] Pitz WJ, Mueller CJ. Recent progress in the development of diesel surrogate fuels. Prog Energy Combust Sci 2011;37:330–50.
[135] Westbrook CK, Pitz WJ, Curran HJ. Chemical kinetic modeling study of the effects of oxygenated hydrocarbons on soot emissions from diesel engines. J Phys Chem A 2006;110:6912–22.
[136] Seiser R, Pitsch H, Seshadri K, Pitz WJ, Curran HJ. Extinction and autoignition of *n*-heptane in counterflow configuration. Proc Combust Inst 2000;28:2029–37.
[137] Patel A, Kong SC, Reitz RD. Development and validation of a reduced reaction mechanism for HCCI engine simulations. SAE Paper 2004-01-0558; 2004.
[138] Wang H, Jiao Q, Yao M, Yang B, Qiu L, Reitz RD. Development of an *n*-heptane/toluene/PAH Mechanism and its application for combustion and soot prediction. Int J Engine Res 2013.
[139] Ogink R, Golovitchev V. Gasoline HCCI modeling: computer pogram combining detailed chemistry and gas exchange processes. SAE Paper 2001-01-3614; 2001.
[140] Zheng J, Yang W, Miller DL, Cernansky NPA. Skeletal chemical kinetic model for the HCCI combustion process. SAE Paper 2002-01-0423; 2002.
[141] Mehl M, Chen JY, Pitz JW, Sarathy SM, Westbrook CK. An approach for formulating surrogates for gasoline with application toward a reduced surrogate mechanism for CFD engine modeling. Energy Fuels 2011:5215–23.
[142] Smith GP, Golden DM, Frenklach M, Moriarty NW, Eiteneer B, Goldenberg M, et al. GRI-Mech 3.0. URL: 〈http://www.me.berkeley.edu/gri_mech〉; 2006.
[143] Sato S, Yamasaki Y, Kawamura H, Iida N. Research on the influence of hydrogen and carbon monoxide on methane HCCI combustion. JSME Int J B—Fluid Therm Eng 2005;48:725–34.

[144] Msaad AA, Belcadi A, Mahdaoui M, Aaffad E, Mouqallid M. Reduced detailed mechanism for methane combustion. Energy Power Eng 2012;4:28–33.
[145] Slavinskaya NA, Wiegand M, Starke JH, Riedel U, Haidn OJ, Suslov D. Kinetic mechanism for low-pressure oxygen/methane ignition and combustion. Prog Propuls Phys 2013;4:707–32.
[146] Marinov NM, Westbrook CK, Pitz WJ. Detailed and global chemical kinetics model for hydrogen. In: Proceedings of the 8th international symposium on transport properties. San Francisco; 1995.
[147] Burke MP, Chaos M, Ju YG, Dryer FL, Klippenstein SJ. Comprehensive H_2/O_2 kinetic model for high-pressure combustion. Int J Chem Kinet 2012;44:444–74.
[148] Herbinet O, Pitz WJ, Westbrook CK. Detailed chemical kinetic mechanism for the oxidation of biodiesel fuels blend surrogate. Combust Flame 2010;157:893–908.
[149] An HJ, Wilhelm WE, Searcy SW. Biofuel and petroleum-based fuel supply chain research: a literature review. Biomass Bioenergy 2011;35:3763–74.
[150] Amin S. Review on biofuel oil and gas production processes from microalgae. Energy Convers Manag 2009;50:1834–40.
[151] Hughes KJ, Turanyi T, Clague AR, Pilling MJ. Development and testing of a comprehensive chemical mechanism for the oxidation of methane. Int J Chem Kinet 2001;33:513–38.
[152] Huang J, Bushe WK. Experimental and kinetic study of autoignition in methane/etliane/air and methane/propane/air mixtures under engine-relevant conditions. Combust Flame 2006;144:74–88.
[153] Lu T, Law CK. An efficient reduced mechanism for methane oxidation with NO chemistry. In: Proceedings of the 5th US combustion meeting. San Diego; 2007.
[154] O Conaire M, Curran HJ, Simmie JM, Pitz WJ, Westbrook CK. A comprehensive modeling study of hydrogen oxidation. Int J Chem Kinet 2004;36:603–22.
[155] Zhukov VP. Verification, validation, and testing of kinetic mechanisms of hydrogen combustion in fluid-dynamic computations. ISRN Mech Eng 2012;2012:11.
[156] Marinov NM. A detailed chemical kinetic model for high temperature ethanol oxidation. Int J Chem Kinet 1999;31:183–220.
[157] Lindstedt RP, Meyer MP. A dimensionally reduced reaction mechanism for methanol oxidation. Proc Combust Inst 2002;29:1395–402.
[158] Mosbach S, Kraft M, Bhave A, Mauss F, Mack JH, Dibble R. Simulating a homogeneous charge compression ignition engine fuelled with a DEE/EtOH blend. SAE Paper 2006-01-1362; 2006.
[159] Gail S, Thomson MJ, Sarathy SM, Syed SA, Dagaut P, Dievart P, et al. A wide-ranging kinetic modeling study of methyl butanoate combustion. P Combust Inst 2007;31:305–11.
[160] Brakora JL, Ra Y, Reitz RD, McFarlane J, Daw SC. Development and validation of a reduced reaction mechanism for biodiesel-fueled engine simulations. SAE Paper 2008-01-1378; 2008.
[161] Luo ZY, Plomer M, Lu TF, Som S, Longman DE, Sarathy SM, et al. A reduced mechanism for biodiesel surrogates for compression ignition engine applications. Fuel 2012;99:143–53.
[162] Sarathy SM, Vranckx S, Yasunaga K, Mehl M, Osswald P, Metcalfe WK, et al. A comprehensive chemical kinetic combustion model for the four butanol isomers. Combust Flame 2012;159:2028–55.
[163] Brakora J, Ra Y, Reitz R. Combustion model for biodiesel-fueled engine simualtions using realistic chemistry and physical properties. SAE paper 2011-01-0831; 2011.
[164] Fiveland SB, Assanis DN. Development of a two-zone HCCI combustion model accounting for boundary layer effects. Homogeneous charge compression ignition (HCCI) combustion. Michigan: SAE Paper 2001-01-1028; 2001.
[165] Aceves SM, Flowers DL, Westbrook CK, Smith JR, Pitz W, Dibble R, et al. A multi-zone model for prediction of HCCI combustion and emissions. Compression ignition combustion processes. Michigan: SAE Paper 010327; 2000.
[166] Liu Z, Chen RA. Zero-dimensional combustion model with reduced kinetics for Si engine knock simulation. Combust Sci Technol 2009;181:828–52.
[167] Aceves SM, Martinez-Frias D, Flowers D, Espinosa-Loza F, Dibble R, Christensen M, et al. Piston-liner crevice geometry effect on HCCI combustion by multi-zone analysis. Powertrain & fluid systems. San Diego: SAE Paper 2002-01-2869; 2002.
[168] Babajimopoulos A, Assanis DN, Fiveland SB. An approach for modeling the effects of gas exchange processes on HCCI combustion and its application in evaluating variable valve timing control strategies. SAE Paper 2002-01-2829; 2002.
[169] Puduppakkam KV, Liang L, Naik CV, Meeks E, Bunting BG. Combustion and emissions modeling of a gasoline HCCI engine using model fuels. SAE Paper 2009-01-0669; 2009.
[170] Puduppakkam KV, Naik CV, Wang C, Meeks E. Validation studies of a detailed kinetics mechanism for diesel and gasoline surrogate fuels. SAE Paper 2010-01-0545; 2010.
[171] Dec JE. Advanced compression-ignition engines-understanding the in-cylinder processes. Proc Combust Inst 2009;32:2727–42.
[172] Sjoberg M, Dec JE, Babajimopoulos A, Assanis D. Comparing enhanced natural thermal stratification against retarded combustion phasing for smoothing of HCCI heat-release rates. SAE Paper 2004-01-2994; 2004.
[173] Maurya RK, Agarwal AK. Experimental study of combustion and emission characteristics of ethanol fuelled port injected homogeneous charge compression ignition (HCCI) combustion engine. Appl Energy 2011;88:1169–80.
[174] Hou JX, Qiao XQ, Wang Z, Liu W, Huang Z. Characterization of knocking combustion in HCCI DME engine using wavelet packet transform. Appl Energy 2010;87:1239–46.
[175] Komninos Kosmadakis. Heat transfer in HCCI multi-zone modeling: Validation of a new wall heat flux correlation under motoring conditions. Appl Energy 2011;88:1635–48.
[176] Jia M, Xie M, Peng ZA. A comparative study of multi-zone combustion models for HCCI engines. SAE Paper 2008-01-0064; 2008.
[177] Reitz RD, Han Z. A temperature wall function formulation for variable-density turbulent flows with application to engine convective heat transfer modeling. Int J Heat Mass Transf 1997;40:613–25.
[178] Soyhan HS, Yasar H, Walmsley H, Head B, Kalghatgi GT, Sorusbay C. Evaluation of heat transfer correlations for HCCI engine modeling. Appl Therm Eng 2009;29:541–9.
[179] Tennekes H, Lumley JLA. First course in turbulence. United States of America: The MIT Press; 1972.
[180] Peters N. Turbulent combustion. 1st ed.. Cambridge: Cambridge University Press; 2000.
[181] Cant RS, Mastorakos E. An introduction to turbulent reacting flows. London: Imperial College Press; 2008.
[182] Aceves SM, Flowers DL, Martinez-Frias D, Espinosa-Loza F, Christensen M, Johansson B, et al. Analysis of the effect of geometry generated turbulence on HCCI combustion by multi-zone modeling. SAE Paper 208614; 2004.
[183] Combustion; 2009. URL: 〈http://www.cfd-online.com/Wiki/Combustion〉 [accessed 06.05.11].
[184] Janicka J, Sadiki A. Large eddy simulation of turbulent combustion systems. Proc Combust Inst 2005;30:537–47.
[185] Alfonsi G. Reynolds-Averaged Navier-Stokes Equations for Turbulence Modeling. Appl Mech Rev 2009;62:040802.
[186] Girimaji SS. Partially-averaged Navier-Stokes model for turbulence: a Reynolds-averaged Navier-Stokes to direct numerical simulation bridging method. J Appl Mech—Trans ASME 2006;73:413–21.
[187] Sone K, Menon S. Effect of subgrid modeling on the in-cylinder unsteady mixing process in a direct injection engine. J Eng Gas Turb Power 2003;125:435–43.
[188] Tkatchenko I, Kornev N, Jahnke S, Steffen G, Hassel E. Performances of LES and RANS models for simulation of complex flows in a coaxial jet mixer. Flow Turbul Combust 2007;78:111–27.
[189] Tucker PG. Computation of unsteady internal flows. Dordrecht: Kluwer Academic; 2001.
[190] Celik I, Yavuz I, Smirnov A. Large eddy simulations of in-cylinder turbulence for internal combustion engines: a review. Int J Engine Res 2001;2:119–48.
[191] Pitsch H. Large-eddy simulation of turbulent combustion. Annu Rev Fluid Mech 2006;38:453–82.
[192] Haworth DC. Large-eddy simulation of in-cylinder flows. Oil Gas Sci Technol 1999;54:175–85.
[193] Benarafa Y, Cioni O, Ducros F, Sagaut P. RANS/LES coupling for unsteady turbulent flow simulation at high Reynolds number on coarse meshes. Comput Method Appl Mech Eng 2006;195:2939–60.
[194] Subramaniam S, Pope SB. A mixing model for turbulent reactive flows based on Euclidean minimum spanning trees. Combust Flame 1998;115:487–514.
[195] Mitarai S, Riley JJ, Kosaly G. Testing of mixing models for Monte Carlo probability density function simulations. Phys Fluids 2005;17:047101.
[196] Villermaux J, Devillon JC. Représentation de la coalescence et de la redispersion des domaines de ségrégation dans un fluide per modéle d'interaction phénoménologique. In: Proceedings of the second international symposia on chemical reaction engineering (ISCRE). Netherlands; 1972. p. B1.
[197] Janicka J, Kolbe W, Kollmann W. Closure of the transport equation for the probability density function of turbulent scalar fields. J Non-Equilib Thermodyn 1979;4:47–66.
[198] Bisetti F, Chen JY. LES of Sandia flame D with eulerian PDF and finite-rate chemistry. In: Combustion Processes Laboratories UB, editor. Combustion modelling. Berkeley: University of California; 2005.
[199] Bisetti F, Chen JY, Hawkes ER, Chen JH. Probability density function treatment of turbulence/chemistry interactions during the ignition of a temperature-stratified mixture for application to HCCI engine modeling. Combust Flame 2008;155:571–84.
[200] Pope SB. PDF method for turbulent reactive flows. Prog Energy Combust Sci 1985;11:119–92.
[201] Haworth DC. Progress in probability density function methods for turbulent reacting flows. Prog Energy Combust Sci 2010;36:168–259.
[202] Bilger RW. Conditional moment closure for turbulent reacting flow. Phys Fluids A—Fluid Dyn 1993;5:436–44.
[203] Schroll P. Conditional moment closure for spray combustion and ignition. Cambridge: University of Cambridge; 2009.
[204] Bushe WK, Steiner H. Conditional moment closure for large eddy simulation of nonpremixed turbulent reacting flows. Phys Fluids 1999;11:1896–906.
[205] Klimenko AY, Pope SB. The modeling of turbulent reactive flows based on multiple mapping conditioning. Phys Fluids 2003;15:1907–25.
[206] Cleary MJ, Kronenburg A. Multiple mapping conditioning for extinction and reignition in turbulent diffusion flames. Proc Combust Inst 2007;31:1497–505.
[207] Wandel AP, Klimenko AY. Testing multiple mapping conditioning mixing for Monte Carlo probability density function simulations. Phys Fluids 2005;17:128105.
[208] Vogiatzaki K, Kronenburg A, Cleary MJ, Kent JH. Multiple mapping conditioning of turbulent jet diffusion flames. Proc Combust Inst 2009;32:1679–85.
[209] Vogiatzaki K, Cleary MJ, Kronenburg A, Kent JH. Modeling of scalar mixing in turbulent jet flames by multiple mapping conditioning. Phys Fluids 2009;21:025105.

[210] Cleary MJ, Klimenko AY, Janicka J, Pfitzner M. A sparse-Lagrangian multiple mapping conditioning model for turbulent diffusion flames. Proc Combust Inst 2009;32:1499–507.
[211] Vaishnavi P, Kronenburg A. Multiple mapping conditioning of velocity in turbulent jet flames. Combust Flame 2010;157:1863–5.
[212] Kronenburg A, Cleary MJ. Multiple mapping conditioning for flames with partial premixing. Combust Flame 2008;155:215–31.
[213] Mastorakos E. Conditional moment closure. Cambridge: University of Cambridge; 2010 ([accessed 05.05.11]).